HHS Public Access

Author manuscript

*Chem Soc Rev*. Author manuscript; available in PMC 2017 March 21.

Published in final edited form as:

*Chem Soc Rev*. 2016 March 21; 45(6): 1750–1780. doi:10.1039/c5cs00914f.

# Biological and environmental interactions of emerging two-dimensional nanomaterials

**Zhongying Wang**[a], **Wenpeng Zhu**[a], **Yang Qiu**[a], **Xin Yi**[a], **Annette von dem Bussche**[b], **Agnes Kane**[*,b,c], **Huajian Gao**[*,a], **Kristie Koski**[*,d], and **Robert Hurt**[*,a,c]

[a]School of Engineering, Brown University, Providence, RI 02912, USA.

[b]Department of Pathology and Laboratory Medicine, Brown University, Providence, RI 02912, USA.

[c]Institute for Molecular and Nanoscale Innovation, Brown University, Providence, RI 02912, USA.

[d]Department of Chemistry, Brown University, Providence, RI 02912, USA.

## Abstract

Two-dimensional materials have become a major focus in materials chemistry research worldwide with substantial efforts centered on synthesis, property characterization, and technological application. These high-aspect ratio sheet-like solids come in a wide array of chemical compositions, crystal phases, and physical forms, and are anticipated to enable a host of future technologies in areas that include electronics, sensors, coatings, barriers, energy storage and conversion, and biomedicine. A parallel effort has begun to understand the biological and environmental interactions of synthetic nanosheets, both to enable the biomedical developments and to ensure human health and safety for all application fields. This review covers the most recent literature on the biological responses to 2D materials and also draws from older literature on natural lamellar minerals to provide additional insight into the essential chemical behaviors. The article proposes a framework for more systematic investigation of biological behavior in the future, rooted in fundamental materials chemistry and physics. That framework considers three fundamental interaction modes: (i) chemical interactions and phase transformations, (ii) electronic and surface redox interactions, and (iii) physical and mechanical interactions that are unique to near-atomically-thin, high-aspect-ratio solids. Two-dimensional materials are shown to exhibit a wide range of behaviors, which reflect the diversity in their chemical compositions, and many are expected to undergo reactive dissolution processes that will be key to understanding their behaviors and interpreting biological response data. The review concludes with a series of recommendations for high-priority research subtopics at the “bio-nanosheet” interface that we hope will enable safe and successful development of technologies related to two-dimensional nanomaterials.

*robert_hurt@brown.edu, huajian_gao@brown.edu
*Agnes_Kane@brown.edu
*koski@brown.edu

## 1. Introduction

The class of two-dimensional (2D) nanomaterials is large and diverse – encompassing monolayer carbons to chalcogenides to layered silicate minerals (Fig. 1). The isolation of graphene[1, 2] and the demonstration of an indirect to direct band gap transition in monolayer $MoS_2$[3, 4] among other findings, have made 2D materials research one of the most exciting fields in science today. For the purposes of this review, we define a 2D material as a single sheet of covalently bonded atoms, arranged in one to several atomic layer planes, of extended lateral dimension that form a high-aspect-ratio (>10) sheet- or plate-like solid. The review scope also includes "2D layered materials" which we define as sheet-like solids that consist of several such covalently bonded layers separated by van der Waals (vdW) gaps, as well as "layered materials", which are bulk substances with lamellar crystal structures that consist of many such covalent layers and associated vdW gaps. For convenience the broad material class will sometimes be referred to in this review using the abbreviated phrase: "2D materials".

The current rate of innovation in 2D materials is very high, but it is important to recognize that this material class is not new to science or industry.[5–12] Chalcogenide, oxide, and graphitic layered materials already find applications in batteries as intercalation electrodes.[13] Boron nitride is used as a lubricant and as a cosmetic additive that imparts optical luster or "shine". The chalcogenides are semiconductors and find use in thermoelectric devices[13] and some oxide layered materials exhibit electrochromic properties, changing color upon electrochemical intercalation.[13] $MoS_2$ has been in use for well over a century as a solid industrial lubricant[13] and a catalyst.[14] The layered mineral, bentonite or montmorillonite, is used as an adsorbent in applications such as cat litter and the packing of nuclear fuels – it is also used as a food additive, giving yogurt its smoothness. These applications have generated considerable knowledge and experience in the environmental health and safety issues for layered materials. While that experience can inform the 2D material field, the complexity and diversity of these emerging materials (see Fig. 1), together with their very rapid rate of development, will require a much more systematic and comprehensive approach to ensure their safety.

### 1.1 The importance of biological and environmental interactions

Much of the current work on 2D materials focuses on basic synthesis, or the characterization of fundamental electronic, photonic, and catalytic behaviors.[15] One may ask what the motivation is for studying behavior in biological systems and the natural environment? First, 2D materials are being actively explored for applications in biology[16] and the environment,[17] and we anticipate these application areas will grow, much in the same way that applications for carbon nanotubes grew far beyond their initial application area of electronic devices as the field matured. Secondly, the study of biological and environmental interactions forms the scientific basis for understanding and managing development risks, which is equally important for biomedical and non-biomedical technologies. The latter inevitably lead to unintended human exposures and environmental releases both from R&D (research and development) activities and larger-scale nano-manufacturing. In our experience, environmental health and safety (EHS) issues are typically raised by parties

outside of science, and an early, proactive approach to risk characterization within the scientific community can benefit all parties by reducing the uncertainties that become barriers to investment and permitting needed for large-scale development and commercialization. One can argue that early-stage research on EHS implications should be an essential task along the development pathway for all new chemical and materials-based technologies, and the 2D material field, as a subset of the larger nanotechnology field, should be a high priority for this type of research over the next decade.

### 1.2 Scope of review and diversity of 2D materials

This review focuses on emerging 2D and layered materials "beyond graphene". This choice was made because the graphene field has already been the subject of several detailed reviews,[18–20] and where the present review does refer to graphene data or behaviors, it is done to inform or guide the thinking on the other 2D materials. We also choose to cover both monolayer (2D) and multilayer (2D layered) forms, as both types will likely be fabricated and commercialized at large scale leading to human and environmental exposures. Relatively little is known about plate-like material interactions with biological systems, and even the thicker multilayer nanomaterials (< 100 nm) may show new and interesting modes of interaction worthy of scientific attention. This review therefore considers all plate-like, high-aspect-ratio (>10) materials with at least one dimension less than about 100 nm (in correspondence with the US federal government definition of nanoscale materials). Where data on the 2D versions are lacking, the review will offer relevant information on bulk lamellar materials, which are often precursors for 2D materials, to give insight into the fundamental chemistry.

A major challenge for the field and for this review is the sheer diversity of this material class (Fig. 1). The numerous chemical compositions and atomic configurations, when crossed with the different physical forms (Fig. 1) lead to an enormous set of new 2D materials for potential study. It will be obvious to readers that understanding biological interactions or quantifying risks by the brute force *in vivo* testing of all relevant 2D materials is not a practical path forward. There is strong motivation to use fundamental materials chemistry and physics to classify the materials into categories to prioritize research and generalize the results of that research wherever possible. Toward this goal, the present review proposes a framework for relating biological responses to fundamental 2D materials chemistry and physics, which we believe will promote a more systematic approach for the 2D material field going forward.

In the remainder of this review, Section 2 gives background information on synthesis, processing and exposure, while Section 3 reviews the available data on biological interactions. Section 4 outlines a proposed framework for the systematic study of biological interactions grounded in materials chemistry and physics, while Section 5 focuses on material behavior in the natural environment. Our conclusions and recommendations are briefly summarized in Section 6.

## 2. Fabrication methods, processing and exposure potential

A central paradigm in toxicology is that risk = hazard (*i.e.* toxicity) x exposure. Modern technology makes use of countless hazardous substances, for which risk is adequately managed by controlling exposure. For the 2D materials field it will be important to understand and anticipate potential exposures as a guide to safe processing, and in order to set research priorities in the area of toxicity evaluation. In general, human exposures are occupational, environmental, or biomedical, as shown in Fig. 2. Occupational exposures are occurring now for R&D workers and will become increasingly important for workers in nano-manufacturing industries as the field evolves. In occupational settings workers are typically exposed to materials in their as-produced form, or to manufacturing intermediates or byproducts (see below), and the importance of these exposures provides motivation for studying the biological interactions of primary 2D materials in their as-produced form. Environmental exposures, in contrast, occur after the uncontrolled release of materials, which often undergo chemical transformation to other forms before returning to humans through air, food, or water (see Section 5). Biomedical exposures are potentially important, but occur in more controlled settings, and their management is already an integral part of drug and biomedical device development.[16] As a first step, it will be useful to briefly consider the most common 2D material synthesis and processing methods that determine the nature of the current and near-term exposures to researchers and process developers.

Several excellent reviews cover synthesis methods for 2D materials including graphene-based materials, oxides, and chalcogenides.[22–25] The very different types of chemical bonding among oxides, halides, nitrides, and chalcogenides result in very different melting points and vapor pressures, which call for different synthesis approaches. While there are a variety of synthetic techniques, most can be categorized as either (i) solution phase (wet chemical) or (ii) vapor phase (Fig. 3). It remains a challenge to directly synthesize many materials in true monolayer form; however, graphene, $MoS_2$,[26] and some of the other transition metal dichalcogenides (TMDs) can be synthesized as high quality monolayer sheets.[27] Few-layer materials can often be generated through exfoliation either after synthesis of a layered parent material or through exfoliation of a naturally occurring bulk layered powder.

### 2.1 Solution-based growth

Wet chemical approaches can be used to synthesize 2D materials with thicknesses ranging from the monolayer to hundreds of layers[28, 29] and have several advantages. Reaction temperatures are much lower than in vapor-phase routes, and the products can exhibit exceptional uniformity and low defect density. Materials can be doped during growth by addition of other reagents, and the material surface can be capped using ligand chemistry for surface modification and protection.[27, 30, 31] Solution-based methods may become more prevalent as 2D material technologies move into the commercialization phase because they are often easily translated into larger-scale manufacturing processes. By selection of environmentally benign precursors and solvents, solution-based methods can be adapted to adhere to principles of green chemistry and manufacturing.[27]

A traditional wet-chemical approach to chalcogenides involves hydrothermal or solvothermal growth (Fig. 3b). In a typical reaction, the precursors, solvent, and a reducing agent are sealed in a Teflon-lined steel autoclave (Fig.3b) and held at modest temperatures (< 250°C) for hours to days.[31, 34–36] Materials synthesized in this manner tend to be thinner (contain fewer layers) than some other methods. Examples of layered $Bi_2Se_3$ synthesized solvothermally (1–5 layers) and $MoO_3$ synthesized hydrothermally (~10nm thick) are shown in Fig. 3d and 3e, respectively.[30, 32]

Colloidal synthesis (Fig. 3c) is a well-established technique for fabrication of chalcogenide and oxide nanomaterials.[27] It can also be used to obtain large platelets of layered materials with lateral dimensions ranging from nanometers to ~0.5 micron.[27, 37] An excellent review by Han *et al.* details the variety of wet chemical routes.[27] Layered materials are generated through either injection of a cold solution of precursor chemicals into a hot solvent, similar to other colloidal synthetic routes, or through a one-pot route where precursors are combined and heated (up to 320 °C). Recently, Yoo *et al.*[38] showed a novel colloidal route to generate monolayer dichalcogenides such as $TiS_2$, $HfS_2$, and $ZrS_2$ through a technique referred to as "diluted chalcogen continuous influx". In this method, one controls the rate of delivery of a chalcogen source (such as $H_2S$ or $CS_2$) to a transition metal halide precursor in solution. The rate of chalcogen influx is controlled to be slow enough to favor lateral (2D) growth over 3D growth. Large sheets of 0.2–0.5 μm in lateral dimension can be grown directly from solution.[38]

### 2.2 Vapor-phase growth

Vapor phase growth of 2D materials yields large, high quality single crystals of oxide and chalcogenide materials with morphologies ranging from nanoribbons to plates to monolayers.[23, 39, 40] An excellent review of the current state of the art can be found in Chhowalla *et al.*[15] In a typical vapor-phase process (Fig. 3a), source powder(s) or molecular precursor in solution are heated. A carrier gas (*e.g.* argon, nitrogen, or forming gas) transports the vapor-phase precursors downstream to substrates that are placed in a region of appropriate temperature for nucleation of the layered or 2D material. Optimization of substrate choice, molecular precursors, and reaction geometry can facilitate growth of monolayers. An example of a quartz tube setup for vapor-phase growth is shown in Fig. 3a along with $Si_2Te_3$ generated through large area vapor-solid growth shown in Fig. 3f.[33]

### 2.3 Exfoliation

Exfoliation refers to a class of natural or synthetic processes in which thin flakes are derived from bulk materials either through surface shedding or bulk splitting into sheet-like fragments. In contrast to the growth-based methods above, exfoliation is a top-down assembly method that is primarily physical, though chemical driving forces are sometimes used to drive the physical separation. When used for 2D material synthesis, the precursors are most commonly bulk layered materials, but can also be multilayer products of the above growth processes. Exfoliation has long been used to prepare thin samples for transmission electron microscopy,[41, 42] and happens naturally in the environment with rock weathering of layered materials.[43]

To exfoliate a layered material, some external or internal driving force is needed to overcome or weaken the van der Waals forces between adjacent layers. This can proceed mechanically through friction or shear forces, or chemically through intercalation, where the driving force is provided by the free energy of the intercalation reaction or by electrochemical energy added externally to drive ion intercalation. Exfoliated sheets must typically be stabilized to prevent aggregation and re-stacking using surfactants, polymers, solvents, or liquid-liquid interfaces that trap and stabilize the exfoliated sheets.[15, 44–46]

The isolation of graphene from graphite using scotch tape was the original spark that ignited interest in 2D materials. This type of dry mechanical exfoliation suffers from low-yield and contaminates monolayer surfaces with the adhesive polymer, but has high reproducibility and is quite suitable for making single devices for research purposes and works for all layered materials.[1, 2, 47] Recently, large-area mechanical exfoliation has been demonstrated in $MoS_2$ by exploiting the chemical affinity of sulfur to gold. The chalcogenide is deposited on a gold substrate; top layers are removed by thermal adhesive tape leaving behind a large monolayer.[48] The limitations on throughput can be overcome by exfoliation in the liquid phases.[15, 45, 46, 49] In general, direct sonication of a layered host is carried out in a solvent chosen to stabilize the exfoliated sheets and sometimes selected based on matching surface tension to solid surface energies. While this method can partially exfoliate chalcogenide and oxide systems into few-layer materials, it does not typically provide high yields of the monolayer form. Exfoliated chalcogenides can also be stabilized in solution against reaggregation with ionic surfactants such as sodium cholate[46] or alkyl-trichlorosilanes, which form self-assembled monolayers on the chalcogenide surface.[50] Layered silicates and double layered hydroxides can be exfoliated through a number of routes including ion exchange and swelling of parent compounds.[15, 49, 51]

Electrochemical exfoliation has been used for several decades for exfoliation and restacking of layered materials to generate novel compounds.[13, 22] It proceeds through electrochemical insertion of an ion (such as $Li^+$) into the host crystal.

$$MoS_2 + xLi^+ + xe^- \rightarrow Li_xMoS_2 \quad (1)$$

$$Li_xMoS_2 + xH_2O \rightarrow MoS_2(coll) + (x/2)H_2 + xLiOH(aq) \quad (2)$$

This destabilizes the crystal while also inducing a phase change (Eq. 1). Placing the intercalated material in polar solvents forces hydrolysis of the lithiated species and formation of single-sheet colloidal suspensions which can also be used as-produced or restacked through sandwiching with other materials.[13, 52, 53] The yield of this method is nearly 100% but requires high temperatures, long reaction times, and careful exfoliation to prevent destruction. This method may be one of the most promising for large-scale fabrication of true monolayer materials.[22, 52, 54–57]

### 2.4 Potential for occupational exposure

The nature of the synthesis and processing methods govern the nature of potential occupational exposures. Based on experience with other nanomaterials, a useful distinction can be made between: (a) dry processes (vapor phase growth, dry exfoliation), and (b) wet processes (liquid-phase growth or liquid-phase mechanical or electrochemical exfoliation). Inhalation exposure is a primary concern and occurs most often during dry processing, when CVD reactors are opened, or dry powders are transferred or packaged. Vapor-phase processes that yield substrate-bound films are of less concern than those yielding free powders as primary products. Wet synthesis methods are preferred for managing airborne exposure, but wet growth is often followed by drying to produce powdered products, for which the same issues apply. Exposure issues in wet processing can also arise from spills and splashes, or for spray processing or aerosolization.[58]

There are limited data on airborne concentrations of 2D materials and their respirability, with most of the data on graphene[19, 59] or from human health impact studies of sheet-like silicates (see Section 3). Graphene materials may reach the deep lung despite their large lateral dimension, and the atomic-scale third dimension greatly reduces their aerodynamic diameter and settling behavior.[19, 59] Nanomaterial aerosols are often aggregates, and 2D materials form fundamentally different aggregate structures than 1D materials – they can stack face-to-face into robust, high-density aggregates rather than entangle into low-density spherical aggregates like carbon nanotubes.[60] Research is clearly needed to measure airborne concentrations and identify aggregate structures when emerging 2D materials are subjected to common processing methods. Research is also needed on the respirability of 2D materials and their common aggregate and agglomerate structures.

An underappreciated aspect of 2D material safety is the chemical hazards associated with precursors or byproducts. For both liquid- and vapor-phase processes, toxic gases such as $H_2S$, $H_2Te$, and $H_2Se$ can be used as starting materials or are formed by decomposition during processing or with exposure to water.[61–63] Most vapor phase reactions are carried out in sealed air-free environments, but during high temperature process failure some chalcogenides such as $Bi_2Te_3$ can react violently if exposed to moisture at high temperature. More information is also needed on the byproducts of 2D material synthesis, which must be managed as potential environmental pollutants, as has been pointed out for carbon nanotubes, whose growth intermediates include polycyclic aromatic hydrocarbons.[64]

## 3. Literature review on biological response and risk

This section reviews *in vitro, in vivo* and epidemiological studies relevant to 2D material biological response and risk. In some cases where there are no specific data yet on the 2D monolayer or few-layer forms, we include data on bulk layered materials to provide information on intrinsic chemical toxicity, with the caveat that bulk behavior will not always be a reliable indicator of nanosheet behavior. Because neither *in vitro* studies nor *in vivo* studies in animal models are fully predictive of human disease, we include discussion of known health impacts in workers, and do this for what is arguably the best available case study today – exposure to sheet-like silicates. We begin with general information on material behavior organized by chemical class.

### 3.1 General information by chemical class

**Selenides and tellurides—**The largest class of 2D and layered materials is the chalcogenides (compounds containing S, Se, Te, or Po). Se and Te have various oxidation states from −2 to +6 in even numbers, and appear in several layered material states (Fig. 1). Upon dissolution or decomposition, these materials can release free Se or Te species (see Section 4.1), which are known toxicants for humans and environmental organisms. Selenium is an essential trace element in living organisms that include archaea, algae, bacteria, and many eukaryotes, but at higher doses is an established toxicant. Selenium has been implicated in livestock poisoning through a condition incorrectly referred to as "chronic alkali disease",[65] because it was wrongly attributed to alkaline salts in the soil.[66] Chronic selenium poisoning causes hair loss in the manes and tails of horses, sore hooves in cattle, and poor egg hatchability in fowl.[65] Very high levels of selenium cause blind-stupor and ultimately death in cattle. This condition is common in the several states of the US (Wyoming, South Dakota, Nebraska), where plants can contain up to several thousand ppm of selenium. Tellurium is chemically similar to selenium though more electropositive, more basic, and more metallic. It was noticed that acute tellurium exposure[67] causes suppression of saliva and sweat in humans by paralyzing secretory nerves, similar to atropine. This is usually associated with dryness of the mouth and a metallic taste. Te also causes dilation of capillaries of splanchnic nerves in humans, similar to arsenic. Exposure, in small doses, also leads to somnolence (sleepiness).[67] Tellurium is known to pass the blood-brain barrier and can accumulate in nerve cells.[68] Rabbits injected with tellurium developed dark grey discoloration of the brain after prolonged administration.[68] Injection of tellurium in rats, led to hydrocephalus in their offspring.

In acute selenium or tellurium poisoning, whether through exposure to solid materials or through vapor inhalation, organoselenium species are released as dimethyl selenide, dimethyldiselenide, dimethyl telluride, or dimethylditelluride. This results in a characteristic garlic odor.[65, 69] Microorganisms make methyl-selenide, dimethyl-selenide, dimethyl-diselenide and dimethyl-selenenyl-sulfide with selenium exposure. In some microorganisms this leads to the formation of selenium (0) which can likely bioaccumulate.[69] Exposure to Se and Te can lead to replacement of sulfur in peptides and proteins.[70] Organoselenium and organotellurium byproduct compounds can react with thiol groups from biologically important molecules and oxidize them to disulfides.[71] During synthesis or processing of Se- or Te-based 2D materials, exposure to water or atmospheric moisture can generate $H_2Se$ or $H_2Te$ gases, which have a characteristic odor and are highly toxic.

**Sulfides—**Sulfur is an earth abundant element that is also common in biological systems and not usually associated with toxic effects. For this reason, any health concerns associated with sulfides are likely governed by the metal constituent, or a unique solid-state behavior of the sheet-like compound (Section 4.2). Molybdenum sulfide, $MoS_2$ is currently the most intensely investigated of the 2D materials beyond graphene. It has received enormous attention for the appearance of an indirect to direct band gap transition as it is exfoliated to a monolayer.[4] $MoS_2$ also has several superior catalytic properties for hydrogen evolution and hydrodesulfurization – both properties that are affected by the number of layers of the material.[13] Bulk $MoS_2$ has been an industrial material for over a century, serving as a solid

lubricant. As a mineral, molybdenite, it is a major byproduct of mining and is also major mineral constituent of acid mine drainage.[72, 73] Metal sulfides are formed in geological environments such as a sulfur-heavy, reducing atmosphere. After the process of mining, these metal sulfides often as wastes and including $MoS_2$, are exposed to water, bacteria, and atmospheric oxygen. Slowly, these materials begin to oxidize and in the process generate acidity, for example in the form of sulfur acid.[73] Bacterial activity enhances dissolution of sulfide metals and subsequent creation of heavy metals. This toxic mixture can lead to contamination of groundwater, rivers, and environmental ecosystems. Although most forms of sulfur are not toxic, sulfide-based 2D materials can evolve the toxic gas $H_2S$ during processing, an example being the exposure of the layered phases smithite ($Fe_3S_4$) or mackinawite (FeS) to mild acids.[74]

**Oxides—**Only a few of the 2D materials in Figure 1 are oxides, and some of these have polymorphs that are not simply layered. As an example, lead oxide has two polymorphs; of these only the tetragonal α-PbO (litharge, yellow lead) is a layered material. Many transition metal oxides are reactive and potentially toxic in nanoparticle form, as they exhibit increasing catalytic activity and dissolution rates at small sizes. Micron-sized vanadium pentoxide ($V_2O_5$) is a layered material with notable toxicity, landing it on the EPA "p-list" of acutely hazardous chemicals. It exhibits unique chromic properties and has been investigated as a lithium ion battery electrode material.[13] Bulk $V_2O_5$ is also used as a catalyst in industry – for example in the manufacture of sulfuric acid and steel alloys, and is a byproduct of petroleum processing.[75] Emissions of $V_2O_5$ from natural sources such as volcanoes, sea salt spray, forest fires, and other biogenic processes has been estimated at 8.4 metric tons annually.[76–78] As a layered material, bulk $V_2O_5$ has been the subject of numerous biological response studies. It is genotoxic,[79] and causes destruction of the testicular and liver architecture in male guinea pigs, and has been reported to be a developmental toxicant in mice.[80] To our knowledge, there is no specific data on the 2D (exfoliated) forms of $V_2O_5$.

Molybdenum trioxide, $MoO_3$, exhibits similar chromic properties to $V_2O_5$, changing color from transparent white to blue upon intercalation in the bulk form.[13] It is important in the 2D field, standing out as the layered precursor for many $MoS_2$ growth methods.[26] Bulk molybdenum oxide itself is an industrial byproduct from the metal alloy industry, and is used as a catalyst and a pigment. Ingested as a solid, bulk $MoO_3$ powders are fatal to rats and guinea pigs at 1200 to 6000 mg, which is a high dose, while inhalation of its vapor does not lead to fatality,[81] Nanoscale $MoO_3$ also exhibits anti-bacterial and anti-fouling properties,[82] which suggests its future use in marine paints or coatings.

**Oxyhalides—**Oxychloride materials have received little attention in the 2D field though several synthetic routes exist to create nanosheet forms.[83, 84] Layered bismuth oxychloride is used in some cosmetics for its appearance, where it is referred to as "synthetic pearl". Before the arrival of antibiotics, it was used to treat syphilis.[85] No carcinogenicity is observed following ingestion of large quantities of bulk bismuth oxychloride by rats.[86] Another common layered oxychloride is AlOCl, which is now used commercially as in antiperspirant formulations.

**Metal toxicity—**Most of the 2D materials in Figure 1 contain metallic elements, which upon dissolution or degradation (Section 4.1) can induce biological responses characteristic of the element and its soluble species. Because of the diverse sources of metal contamination in the environment, many of these effects have been well characterized and the subject of extensive reviews on metal toxicity.[87–92] Metals or metalloids found in 2D materials include well-known toxicants such as Hg, Pb, and As with their own extensive literature on environmental and human health effects. Among the most common metals found in emerging 2D materials are molybdenum, tungsten, manganese, vanadium, bismuth, and nickel. Molybdenum is an essential trace element for both animals and plants, and in mammals is incorporated in certain metalloflavoproteins.[93] Molybdate is also an antioxidant and has been tested for treatment of diabetes in animal models.[94] In plants, it is necessary for fixing of atmospheric nitrogen by bacteria at the start of protein synthesis. Molybdenum ions have relatively low toxicity, but mobilization and extracellular release of cadmium, nickel, and chromium ions are of concern because they are lung carcinogens.[95, 96] Vanadium compounds are cofactors for several enzymes, although vanadium salts can inhibit phosphatases, protein kinases, and ribonucleases.[97] On the other hand, vanadium salts are important for iron, thyroid, and cholesterol metabolism and have been proposed for treatment of diabetes and cancer.[98] Similar to vanadate, sodium tungstate has been shown to be effective in animal models of diabetes.[99] However, soluble sodium tungstate administered chronically to rats has been shown to induce oxidative stress in the brain and neurobehavioral changes.[100, 101] Heavy metal tungsten alloy particles are used as a less toxic alternative for depleted uranium for military applications. However, these particles have been shown to induce acute oxidative stress and lung toxicity following intratracheal instillation in rats.[102] Tungsten carbide cobalt (WC-Co) particles are known to induce hard metal lung disease associated with fibrosis or scarring and lung cancer following occupational exposure.[103] In an *in vitro* model using human lung epithelial cells, nano-WC-Co particles were more toxic than micro-WC-Co particles.[104] Implantation of heavy metal tungsten alloy pellets into rat muscles produced aggressive tumors at the implantation site.[105] Manganese is an essential element important for brain glutamate metabolism, energy metabolism, immune function, and growth of bone and connective tissues.[90, 91] $Mn^{+3}$ is more toxic than $Mn^{+2}$ or $Mn^{+4}$ and is redox active.[92] High levels of manganese accumulate in the brain following inhalation by humans associated with a Parkinson-like disease.[106] Metallic bismuth is used as a lead substitute and there is concern about potential toxicity following occupational exposure. In comparison to lead, repeated oral doses in rats produced minimal toxicity up to 1,000 mg/kg.[107] Bismuth salts and colloidal compounds have been widely used in humans for treatment of skin lesions, syphilis, and gastrointestinal disorders. Due to limited absorption and low solubility, these compounds have low toxicity when tested using *in vitro* cellular toxicity assays at doses up to 100 μM.[108] Bismuth has a low toxicity for a heavy metal, but is known to bioaccumulate in algae.[109]

### 3.2 *In vitro* and *in vivo* studies

Table 1 summarizes the current literature on the biological response to 2D materials, including oxides, hexagonal boron nitride (h-BN), and metal chalcogenides. Bulk $MoS_2$ materials are generally regarded to have low toxicity,[110] and only recently have studies begun to address the 2D forms. Teo *et al.*[111] compared the toxicity of exfoliated versions of

transition metal dichalcogenides with three different chemical compositions: $MoS_2$, $WS_2$ and $WSe_2$. The studies using lung epithelial cells (A549) concluded that all three materials showed low cytotoxicity up to 100 μg/ml, and that $WSe_2$ nanosheets alone began to show toxicity above 200 μg/ml. Since $WS_2$ and $WSe_2$ nanosheets both contain tungsten, the data suggest that the adverse effects of $WSe_2$ nanosheets at high dose are related to the specific chalcogen: Se. Chng *et al.*[112] pursued a different question by studying a single chemistry ($MoS_2$) but using a variety of preparation methods to compare $MoS_2$ materials with different degrees of exfoliation (thickness/layer-number). Similar to Teo *et al.*, they report low toxicity in all versions of 2D exfoliated $MoS_2$, but do see cytotoxicity at high doses (above about 100 μg/ml) and the most cytotoxic materials are those with higher degrees of exfoliation (fewest layers). The cytotoxicity trends may reflect a fundamental effect of thickness (*e.g.* membrane damage caused by atomically thin edges in the most exfoliated samples) or elevated surface area.[112] The discussion in Section 4.1 suggests such area effects in $MoS_2$ may be related to increased rates of oxidative dissolution leading to increased concentrations of free molybdenum species. Wang *et al.*[110] also report low cytotoxicity for several different formulations of $MoS_2$ nanosheets, but go on to show that aggregating the nanosheets by flocculation increases pro-inflammatory responses both *in vitro* and in the mouse lung. This study suggests that "2D–$MoS_2$ nanomaterials are relatively safe" and that their safety is promoted in formulations that ensure good dispersion. Shah *et al.*[113] also report no loss of viability in cells exposed to few-layer $MoS_2$ nanosheets at doses up to 100 μg/ml. All of these studies use $MoS_2$ nanosheets of small lateral dimension (< 1 μm and typically < 200 nm), so the important issue of size effects, and the increased biological response to materials with large lateral dimension as reported for graphene-based materials,[19, 20, 114, 115] remains unexplored for these other 2D materials (see section 4.2).

Antimicrobial activity of 2D graphene oxide nanomaterials and nanocomposites has been linked to their shape, dimensions, chemical composition, and surface properties.[116] There is very limited information on the antibacterial activity of other emerging 2D nanomaterials. The geometry of nanomaterials has been reported to alter phototoxicity and bacterial killing by nano-$TiO_2$ with nanosheets and nanotubes exhibiting lower phototoxicity than nanorods or nanospheres. However, alignment of nanosheets at the bacterial surface also impacted toxicity[117] similar to graphene oxide sheets of large lateral dimension.[118] A study performed by Fan *et al.*[119] focused on environmental applications using 2D $MoS_2$ to evaluate antibacterial activity. In this work the antimicrobial performance of exfoliated 2D $MoS_2$ versus annealed 2D $MoS_2$ in combination with EDTA was examined. This study revealed that the restacked exfoliated $MoS_2$, which differs in phase composition from the exfoliated $MoS_2$, leads to a significantly greater inactivation of *Escherichia coli* biofilm production then the annealed $MoS_2$. Higher electron conductivity of 2D $MoS_2$ leads to increased generation of reactive oxygen species and toxicity to both planktonic bacteria and mature biofilms without causing significant toxicity in eukaryotic cells. In this regard exfoliated $MoS_2$ in combination with EDTA has similar potential as graphene oxide composites for water treatment applications and inhibition of biofilm formation as described previously.[120] Krishnamoorthy *et al.*[121] showed that $MoO_3$ platelets cause toxicity in 4 different bacteria strains, due to physical disruption of bacterial cell walls with potential application as an antibacterial agent.

Studies on biomedical applications often contain some relevant information on toxicity/biocompatibility. Kou *et al.*[122] report low cytotoxicity for 2D $MoS_2$, coated with PEG/PEI as a carrier for gene delivery. Liu *et al.*[123] showed that $MoS_2$ and $MoS_2$-PEG nanosheets do not cause significant toxicity in HeLa cells at concentrations up to 0.16 mg/ml for 24 hrs, and that plain $MoS_2$ causes only a slightly increased toxicity at day 2 and 3 (around 80% and 73% viability) versus 90% viability in $MoS_2$-PEG nanosheet-exposed HeLa cells at this concentration. PEGylated $TiS_2$ nanosheets are reported to have low cytotoxicity in a murine breast cancer cell line up to a concentration of 0.1 mg/ml for 24 hrs.[124] Zhang *et al.*[125] explored polymer-coated $Bi_2Se_3$ nanosheets (50 nm × 6 nm) as tumor inhibitors and contrast agents due to the high atomic number of Bi (see Fig. 4). Direct injection in mice at doses up to 20 mg/kg produced no obvious adverse effects on growth or changes in body weight up to 90 days, and a panel of measurements focused on immune response, hematology, and biochemistry suggested "limited biological damage".[125] This study focused on biokinetics and showed clearance of the elemental Bi and Se over time scales from 2 – 90 days, and also reported the instability of $Bi_2Se_3$ nanosheets to oxidation as a dry powder in air or in cell culture medium (see Section 4.1).

Song *et al.*[126] report low toxicity for $TiO_2$ nanosheets following intraperitoneal injection into mice, but also report particle accumulation in the liver, leading to minor abnormalities after prolonged exposure times. Tran *et al.*[127] report that $MoO_3$ nanosheets induce toxicity in the breast cancer cell line MCF7 by activation of the caspase pathway, but not in keratinocytes (HaCAT cells), suggesting possible applications in the treatment of breast cancer. $MoO_3$ platelets have also been reported to be toxic to bacteria.[82] In an exploration of $MnO_2$ nanoplates as MRI contrast agents, a significant decrease of cell viability was reported in the breast cancer cell line MCF-7 suggesting that doses will need to be limited to avoid cell damage.[128]

### 3.3 Human health impacts of 2D materials – a case study on sheet-like silicates

The largest body of data on human health effects associated with exposure to sheet-like materials comes from decades of experience in the mining, manufacturing, and applications of naturally occurring sheet-like silicates. Reviewing this literature may help us anticipate the issues that may arise with occupational exposure to the broader set of emerging 2D synthetic materials. The most important class of natural 2D silicate minerals are clays, which are composed of tetrahedral and octahedral sheets based on $SiO_4$ tetrahedra as the basic unit. Kaolinite ($Al_2Si_2O_5(OH)_4$) for example, is a 1:1 layer silicate with a sheet of $SiO_4$ tetrahedra bonded to an octahedral sheet of $Al(OH)_6$ (Fig. 5b). Tetrahedral sheets bonded to an octahedral sheet on both sides are 2:1 layer silicates. The covalently bonded layers are separated by a hydrated gap that contains cations such as $K^+$ in mica and $Mg^{2+}$ or $Ca^{2+}$ in vermiculite.[137] The octahedral and tetrahedral sheets are called platelets, each approximately 0.1 – 0.5 μm in lateral dimension and 1 nm thick usually stacked in multiple layers,[138] and in this regard have very similar dimensions to the emerging 2D synthetic materials. Clays are frequently used as composites in the building industry, in agriculture and in manufacturing of paper, plastics and ceramics.

Bulk unprocessed sheet silicates (*e.g.* vermiculite) may be 100–1000 μm in lateral dimension,[141] and can be delaminated producing nanoplates ~ 0.2 – 10 μm in lateral dimension and 10–40 nm thick[142] using chemical exfoliation, sonication, or thermal shock.[141] Chemical exfoliation of vermiculite into single silicate crystals was reported by Walker and Garrett using ion intercalation to produce swollen crystals that can be disrupted by shearing.[137] These single silicate monolayers can be deposited on a flat surface and stripped off as very strong, flexible films; however, these 2D sheets have not been exploited commercially.

Similar to emerging 2D materials, some sheet-like silicates can roll up into fibrils to create 1D structures, and some of these pose serious human health concerns. Chrysotile asbestos is a 1:1 layer silicate that is rolled up in a spiral to form fibrils (Fig. 5a). These fibrils aggregate into bundles or fibers ~ 25 nm in diameter and up to 40 μm long[143] that are highly flexible, long, and thin. Chrysotile asbestos fibers are very strong, chemically inert, heat resistant, and non-conducting and are widely used in roofing, insulation, tiles, wall board, and reinforcement for concrete.[144]

In contrast to these sheet-like and fibrous silicates, pure $SiO_2$ is an abundant mineral that occurs as crystalline silica or α-quartz or as amorphous silica.[145] Crystalline silica is used in concrete, mortar, porcelain, paints, and abrasives.[145] Amorphous silica lacks the fixed geometric spatial orientation of crystalline silica. Synthetic amorphous silica is produced as a gel, thermal or fumed silica, or chemically modified, precipitated silica and used as fillers in the rubber industry, carriers in agrochemicals, paints, adhesives, inks, and cosmetics.[146]

Pneumoconiosis is a general term used to describe reactions of the lungs to dust inhalation that range in severity (Table 2) depending on the composition of the dust, dose, and duration of exposure.[147] Mining, milling and processing of spherical and fibrous silicate minerals is a well-recognized occupational hazard. Crystalline silica or α-quartz represents 12 wt % of the earth's surface. Rocks containing crystalline silica may have associated impurities, most commonly Al, Fe, and Ti. Inhalation of some sheet silicates has been associated with pneumoconiosis; however, naturally-occurring silicates are frequently contaminated with crystalline silica or asbestos fibers. The lung reactions to these mixtures have been named "mixed-dust pneumoconiosis" and occur in workers exposed to talc contaminated with crystalline silica or asbestos fibers[148] and to mica or kaolinite contaminated with crystalline silica.[149] Case reports of workers exposed to prolonged high levels ( ≥5 $mg/m^3$) of pure talc, mica, or kaolinite who develop silicate pneumoconiosis have been published.[148, 150] Other sheet silicates such as vermiculite are not associated with pneumoconiosis; however, a vermiculite mine in Libby, Montana is contaminated with asbestos fibers that are responsible for asbestosis or fibrosis of the lungs, fibrotic pleural plaques, lung cancer, and malignant mesothelioma in the vermiculite miners and residents.[151, 152] Asbestos fibers are not readily cleared following inhalation and cause severe diseases of the lungs and pleural linings surrounding the lungs in contrast to wollastonite, a highly soluble fibrous silicate that is not associated with lung or pleural disease (Table 2). Inhalation of crystalline silica particles, but not amorphous silica, is also associated with development of lung fibrosis and cancer (Table 2);[146] amorphous silica has a high surface area and dissolves more rapidly than crystalline silica, which is very biopersistent.[153] The crystal lattice of α-quartz is a network of

tetrahedral $SiO_2$ units (Fig. 5c). Crushing or mining of crystalline silica fractures the crystal into small fragments in the micron size range which are respirable and have highly reactive dangling bonds at the surface.[140]

Sheet silicates may pose a potential health risk to workers because these exfoliated sheets can be less than 5 μm in aerodynamic diameter and are thus respirable, similar to other 2D materials such as graphene.[115] Consumers and end users of commercial products containing sheet silicates typically have low levels of exposure and no significant health risks. Minimal toxicity has been shown following oral or dermal exposures in experimental animals.[154] Humans have also been exposed to clay minerals used for food packaging and as pharmaceuticals with no reported toxicity.[138] Clays have been added to the diet to adsorb aflatoxin, a highly toxic and carcinogenic food contaminant.[155] Deliberate ingestion of soils containing clay is called geophagia and may cause nutrient deficiency due to adsorption by clay minerals.[156] Clay minerals and composites are used for medical applications for sustained release in drug delivery, in hydrogels, and in periodontal films;[157] no parenteral toxicity has been shown in experimental animals.[154] However, repeated intravenous injections of drugs containing talc can cause serious inflammation and scarring in the lungs.[158]

Particle toxicity is related to chemical and physical properties of the mineral as well as shape and dimensions that influence lung deposition, clearance, and translocation.[153, 159, 160] In general, particles up to 10μm in diameter can deposit in the alveolar spaces while smaller nanoparticles can penetrate into the lung interstitium and lymphatics and disseminate to distant sites. Macrophages are the primary cellular target of inhaled particles deposited in the conducting airways or alveolar spaces following inhalation. Engulfed particles accumulate in cytoplasmic membrane-bound vesicles called lysosomes where they are degraded by hydrolytic enzymes or stored.[161, 162] Crystalline silica, sheet-liked silicates, and amphibole asbestos fibers are not biodegradable and persist in the lungs, in contrast to amorphous silica or wollastonite fibers that are more soluble and induce only transient inflammation (Table 2). In contrast, chrysotile asbestos is a serpentine silica mineral and the outer layer is brucite – $Mg(OH)_2$, Figure 5a. Under acidic conditions in the lysosomes of macrophages, the outer brucite layer is leached allowing the fibers to split transversely into shorter fibrils that are cleared from the lungs.[153, 163] In general, biopersistent minerals are more likely to induce chronic lung inflammation and fibrosis or scarring. Long, rigid fibrous minerals or large sheet-like silicates are incompletely phagocytized by macrophages [159] and induce formation of aggregates of inflammatory cells or granulomas and fibrosis (Table 2).

Highly toxic mineral particles can damage cellular and lysosomal membranes causing release of mediators that trigger inflammation or cell death.[159, 164] Particle surface properties and surface reactivity, not bulk physical structure or chemical composition, are hypothesized to cause membrane damage in target cells.[153, 165] The surface properties of crystalline silica resulting in lysis of red blood cell membranes (hemolysis) and lysosomal membrane disruption of macrophages are well known. Freshly-fractured crystalline silica exposes Si• and Si-O• dangling bonds on the cleavage planes that react with water to form highly toxic hydroxyl radicals (Fig. 5c)[153, 163] that cause severe acute lung injury in silica miners. Depending on the geographic source and surface contaminants or impurities, aged

crystalline silica is also toxic due to two surface chemical functionalities: silanols or –SiOH groups that form H bonds at neutral pH resulting in membrane disruption and dissociated silanols or siloxane – $SiO^-$ groups that are negatively-charged. This negative surface charge can be masked by $Al^{3+}$, $Zn^{2+}$, or $Fe^{3+}$ ions, and aluminum-containing clays have been shown to reduce the toxicity of α-quartz.[163] In recent comparative studies of a panel of well-characterized bulk and nanoscale silica samples, Pavan *et al.*[166, 167] demonstrated that a defined spatial distribution of silanol and siloxane groups at the particle surface interacts with red blood cell and lysosomal membranes to disrupt their structural integrity resulting in hemolysis or lysosomal membrane destabilization.

In contrast to the well-described mechanisms for membrane reactivity of crystalline silica, the mechanism responsible for induction of hemolysis by sheet like silicates is unclear. Silicates like kaolinite have a net negative surface charge, but also have other functional groups with a positive charge resulting in overall amphoteric properties, depending on pH. Both silica and sheet-like silicate minerals adsorb phospholipids in cell membranes and in surfactant lung lining fluid. Keane and Wallace[164] propose that phospholipid adsorption in the lung lining fluid is initially protective, but that the phospholipid coating is gradually digested in macrophage lysosomes. Differential lung toxicity of crystalline silica and sheet-like silicates may be related to slower rates of lysosomal degradation of adsorbed surfactant lipids. Alternatively, similar to 2D graphene nanosheets of large lateral dimension, sheet-like silicates may be less readily engulfed by macrophages than spherical crystalline silica particles[19] resulting in less extensive lysosomal membrane disruption and lower release of inflammatory mediators. In the case of sheet-like silicate minerals, *in vitro* hemolytic activity is not predictive of *in vivo* toxicity and pathogenicity.

### 3.4 Implication for potential adverse health impacts of emerging 2D nanomaterials

Lessons can be drawn from these historical studies of toxicity of crystalline mineral particles and one-dimensional fibers. First, toxicity depends on surface chemical and mechanical properties, as well as material dimension and shape, and factors like aging and chemical and thermal treatments are important because they influence surface reactivity.[153, 165] Surface chemistry and reactivity have shown to be important for toxicity of amphibole asbestos fibers due to iron-catalyzed generation of reactive oxygen species at the fiber surface.[163] Endogenous biological chelators can mobilize this surface iron enhancing generation of reactive oxygen species in cells and *in vivo*; conversely, deposition of iron and protein onto fiber surfaces may either mask or enhance surface reactivity.[153] Secondly, *in vitro* assays may not be predictive of *in vivo* biological activity if they do not consider *in vivo* surface modifications such as protein and lipid adsorption and subsequent target cell-particle interactions that may lead to additional surface modifications or particle leaching and degradation. Thirdly, we can expect material stability or biopersistence to be an important variable. Long, rigid one-dimensional fibrous particles that are resistant to dissolution can remain in the lungs or translocate to the pleura where they induce both lung and pleural fibrosis and cancer.[168, 169] One-dimensional fibrous or high-aspect ratio nanomaterials are incompletely phagocytized by macrophages and induce lysosomal membrane permeabilization resulting in release of inflammatory mediators and secondary generation of reactive oxygen and nitrogen species by inflammatory cells.[159, 170] Crystalline silica

particles are also highly biopersistent and induce persistent inflammation and reactive species generation that may lead to development of lung cancer.[171, 172]

Finally, the ability of the lung to clear foreign objects is likely to be important, and clearance of 2D materials may be impaired for flakes of large lateral dimension or for large aggregates, as has been shown recently for graphene-based materials.[59, 173, 174] In early data on emerging 2D materials, exfoliated and well-dispersed $MoS_2$ nanosheets were shown to induce less inflammation than aggregated $MoS_2$.[110] It is clear that during these early stages in synthesis, fabrication, and application of these novel 2D nanomaterials and their composites, occupational and environmental exposures must be controlled and carefully monitored to protect the health of workers, end-users, and consumers.

## 4. Fundamental modes of biological interaction

As discussed in Section 1, the extreme diversity in the 2D material family (Fig. 1) presents challenges to any approach that requires *in vivo* testing of each specific material of interest for risk assessment. There is strong motivation to address the problem more systematically through generalized methods or frameworks that group materials into rational classes, and for screening of materials to prioritize them for more detailed examination as part of a tiered testing strategy (*e.g.* see the work by Oberdörster *et al.*[175]) The central premise in this section is that the biological responses to 2D nanomaterials are initiated by material-specific behaviors that can be understood through fundamental materials chemistry and physics. More than a decade of nanotoxicology research focused on particulate and fibrous nanomaterials has provided significant insight into the fundamental chemical and physical basis of these behaviors. Here we propose a framework in which the interactions of 2D materials with biological systems are classified into three basic modes: chemical, mechanical, and electronic (Fig. 6).

*Chemical interactions* occur for materials in non-equilibrium states, which upon immersion in biological fluids undergo reaction or phase transformation that profoundly alters their structure and properties. Of particular importance are oxidative and reductive dissolution processes that release soluble ionic species that are often the primary drivers of adverse biological responses.

*Physical and mechanical interactions* between 2D materials and soft biological structures are governed by mechanical stiffness, surface charge and polarity. Mechanical interactions are of special importance for low-dimensional nanostructures (also known as high-aspect-ratio nanomaterials), which can mechanically perturb soft cellular substructures such as plasma and lysosomal membranes (Fig. 6). For example, long, stiff nanotubes have been implicated in adverse biological responses associated with frustrated cellular uptake and cytotoxicity.[143] In 2D materials, atomically sharp edges can cause spontaneous penetration of cell membranes with low energy barriers and can lead to lipid extraction and membrane damage.[114] Following cellular uptake, low-dimensional materials may cause mechanical stress, deformation, and damage when cells attempt to package large, stiff plate-like or fibrous structures into soft spherical lysosomes.

Finally, 2D nanomaterials can perturb biological process through *electronic and surface redox interactions* (Fig. 6). Permissive electron transfers or H-transfers between material surfaces and biomolecular redox couples in cells and tissue can perturb essential biochemical pathways or initiate new pathways that lead to adverse outcomes such as those mediated by reactive oxygen and nitrogen species. The remainder of Section 4 explores these fundamental interaction modes in more detail.

### 4.1 Chemical interactions and material phase transformations

Over a decade of nanotoxicology research has shown that nanomaterials typically interact with biological systems in chemically specific ways that reflect their unique elemental compositions, phases, and surface chemistries. Immersion of as-produced nanomaterials in biological environments often creates non-equilibrium systems that drive material phase transformations, including oxide formation,[176] sulfidation,[177] selenium/sulfur replacement,[178] degradation, and dissolution driven by oxidation[179] or hydrolysis.[180] Chemical interactions between material surfaces and biological fluid phases also include chemical adsorption of ions, small molecules,[181] proteins,[182] and ligand exchange.[181] Physical transformations such as aggregation, dispersion, settling, and deposition are also important,[183–185] but are not the focus of this review. In some cases, transformations occur in the natural environment prior to exposure (Section 5), and the relevant biological response is not to the original material, but to its transformation products.[186] Even during occupational exposures to freshly prepared materials, transformations can occur in the human body, which at different times interacts with the as-produced material, the final transformation product, and potentially reactive intermediate states that arise during the dynamic transformation process. A variety of phase transformations have been observed in 2D materials, examples including S replacement by Se,[187] or alkali metal intercalation in TMDs, which converts the 2H phase to the metallic 1T phase.[188] Most studies to date have not used physiologically-relevant fluid phases, so the relevance of the reports to biological interactions is unclear. Monolayer and few-layer materials have extraordinarily high surface areas, so biomolecular adsorption, including protein corona formation, is expected to be particularly important, but are also currently unexplored.

Among the possible transformations, dissolution is particularly significant for the biological response, since soluble dissolution products that co-exist with the solid phase have been implicated in the toxic responses for many nanomaterials, including Ag,[178, 189] Cu,[177, 190] ZnO,[191, 192], CdSe,[193] Ni and NiO.[194, 195] The toxicological significance of material dissolution can be rationalized in general terms as a consequence of atomic bioavailability. A toxic metal in particle form interacts with biological molecules only at surface sites, which typically involve a very small fraction of the metal atoms (true in all but the smallest nanoclusters). In contrast, the same metal as free species in solution can be fully bioavailable at the atomic level with each ion or complex able to engage in chemically specific interactions such as thiol binding or redox cycling or metal substitution in enzymes or ion channels. Because dissolution is such a significant transformation, the following section examines dissolution chemistry in detail for 2D materials.

**Dissolution processes for 2D materials—**Biological dissolution is not a simple process -- it often involves solid-phase oxidation or reduction that occurs by rate-limiting chemical reactions with oxidizing or reducing agents in local fluid environments,[196, 197] and the ion release can be promoted or inhibited by biomolecular ligands that complex ions in solution and reduce their chemical potential, or those that bind to and passivate particle surfaces.[177, 196] We start here by considering three distinct dissolution modes: simple (non-redox), oxidative, and reductive (Fig. 7a), and review the existing literature on the basic chemistry of layered materials relevant to these complex processes.

Material dissolution can occur by simple processes that do not involve changes in oxidation state, namely ion dissociation or hydrolysis, often promoted by acidic or basic conditions. Figure 7b shows solubilities by this simple (non-redox) mechanism for an example set of layered materials in simple media at pH 7. Some materials show high solubility and are thus not stable in dilute suspension, and convert completely to soluble forms. Other materials show lower solubilities (in mM range) that may allow the materials to persist in solid form, but will create a co-existing ion pool at mM concentrations, which is sufficient for many metals to show toxic effects (*e.g.* Zn, Ni, Mn[191, 195]). Several materials in Fig. 7b show very low solubilities ($MoS_2$, $MnO_2$), but interestingly these two will be shown to dissolve anyway because they participate in oxidative and reductive pathways respectively (next section).

In Figure 7b, $MoO_3$ and $WO_3$ are known to be thermodynamically unstable and readily hydrolyzed into molybdate and tungstate, respectively (*e.g.* $\mathrm{MoO_3(S)+2OH^{-1} \rightleftarrows MoO_4^{2-}(aq)+H_2O}$) in relatively high pH solution.[198, 199] Thus the equilibrium concentration of $MoO_3$ and $WO_3$ at pH 7 are estimated based on the solubility of sodium molybdate and sodium tungstate, respectively.[200] Acidic conditions have been reported to slow the hydrolysis process of $MoO_3$ since increased proton concentrations shift the above reaction to the left.[201] Below pH ~2, $MoO_3$ is reported to be very stable against hydrolysis.[202] The equilibrium concentration of metal hydroxide (Zn(II), Co(II), Ni(II)), and their corresponding Fe(III)-based LDHs in the form of $M(II)_2Fe(III)(OH^-)_6Cl^-$ are calculated based on published solubility product constants, which indicate the 2D LDHs are even less stable than the corresponding metal(II) hydroxide raising the concerns about their toxicity.[203] Kaolinite and $TiO_2$ have low solubilities and their biological effects are not thought to depend on associated ions.

Fig. 7c and d use oxidation/reduction potentials for layered materials to anticipate the ability of 2D forms to undergo oxidative/reductive dissolution. This presentation follows the approach of Chen and Wang[204] used to predict the ability of compound semiconductors MX (*e.g.* M=Mo, X=$S_2$ in $MoS_2$) to decompose through acquisition or loss of electrons as in the generic half reactions:

$$\mathrm{MX} \rightleftharpoons M^{z+}+X+\mathrm{ze}^-, \varphi^{\mathrm{ox}}=(G(M^{z+})+G(X)-G(\mathrm{MX}))/\mathrm{zeF} \quad \text{(Oxidation)}$$

$$\mathrm{MX}+\mathrm{ze}^- \rightleftharpoons M+X^{z-}, \varphi^{\mathrm{re}}=-(G(M)+G(X^{z-})-G(\mathrm{MX}))/\mathrm{zeF} \quad \text{(Reduction)}$$

where G is the Gibbs free energy of the compound at the standard state, $e$ is the elementary charge and $F$ is the Faraday constant.

This defines the thermodynamic oxidation potential $\varphi^{ox}$ and reduction potential $\varphi^{re}$, which can be obtained from published thermodynamic data.[200, 204, 206–209] A 2D material is thermodynamically able to undergo oxidation in aerobic biological environments if its $\varphi^{ox}$ value is lower (more negative) than that of the oxygen/water redox couple $\varphi(O_2/H_2O)$, and Fig. 7c shows that such oxidation is thermodynamically favorable for TMD materials. Bulk forms of TMDs are reported to be kinetically resistant to complete oxidation due to the formation of a passivating oxide layer,[210], and even TMD thin films require a strong oxidizer and high temperature for their effective etching.[211, 212] It is likely that the ultrathin 2D forms will not form passivating oxide films, and that the oxidative dissolution that is thermodynamically favored (Fig. 7c) would take place readily. Currently dissolution studies on 2D forms are very limited,[213, 214] and experimental research work on this topic deserves to be a high priority.

The reductive pathway to dissolution has received less attention in the nanotoxicology literature. Although biological media contain a variety of reducing agents, little is known about their effects on nanomaterial stability or ion release. Recently, the redox behavior of semiconducting nanomaterials has been correlated with the position of their conduction band edges to the cellular redox potential, which is estimated by the range of potentials in a set of significant biomolecular redox couples.[192] (see Fig. 10). Here we use the cellular redox potential to assess the ability of biological fluids to chemically reduce 2D materials to soluble products. Figure 7d compares the cellular redox range with reduction potentials for an example set of layered materials, and shows that $WO_3$, $MoO_3$ and $MnO_2$ are thermodynamically favored to undergo reductive dissolution. Indeed the literature reports degradation/dissolution of $MnO_2$ nanosheets[16] and this behavior has been used as a tool for intracellular glutathione detection.[215] The reduction kinetics of colloidal $MnO_2$ by cysteine and glutathione have also been studied, and the reaction products were identified as Mn(II) and corresponding disulfide.[216]

Finally, dissolution processes have important implications for biological response and risk. Materials that dissolve readily will be non-biopersistent, and this excludes certain pathogenic responses associated with long-term exposure to persistent particles in the lung or pleura, such as those that give rise to long-latency diseases such as lung fibrosis (asbestosis) or cancer (malignant mesothelioma). On the other hand, dissolution produces soluble species of high-bioavailability that can exert acute toxic effects. The relative importance of these competing effects of dissolution depends sensitively on the intrinsic toxicity of the soluble species, which in turn is closely related to the composition of the 2D material in question. 2D materials that dissolve into low-toxicity species (silicic acid, molybdate anion) can be reasonably anticipated to show low toxicity.

Overall, this review strongly suggests that many 2D materials will undergo biological dissolution (metal chalcogenides, some oxides and hydroxides) in the oxidative, reductive, or simple (non-redox) modes, and will thus not persist in their original solid state. There is critical need to confirm this analysis for monolayer and few-layer materials, and to

characterize the dissolution processes (kinetics and product distributions), which can be coupled with information on the intrinsic toxicity of the soluble products to predict toxicity and manage risk. From a broader perspective, understanding the biological behavior of 2D materials will require much more research on their dynamic evolution in living systems, including not only dissolution, but also degradation, phase transformation, molecular adsorption events, and alterations in physical structure and edge states.

**Surface states and molecular adsorption / exchange—**The extraordinary high surface areas of mono- and few-layer nanosheet materials may not only accelerate dissolution processes, but may also lead to high chemical reactivities and adsorption capacities/rates relative to many other common nanomaterials. The surface chemistry of nanosheet materials must be understood in terms of their 2D geometries. Unlike the reactive, cleaved surfaces of 3D α-quartz (Fig. 5c), cleavage of 2D materials is typically a *physical exfoliation* that does not (necessarily) involve bond rupture and creation of nascent active sites. Nanosheet materials without crystalline defects may be expected to show low reactivities on their basal surfaces for many chemical processes. In contrast, the edge planes of 2D materials often involve unsatisfied valencies, or are decorated by extrinsic functional groups that result from environmental interactions of those unsatisfied bonds during synthesis or processing. This logic might suggest edge-dominated chemical reactivity in 2D materials, but this is not clear due to the large basal/edge ratio that is intrinsic to high-aspect-ratio sheet mono- or few-layer sheets (e.g. those of extended lateral dimension). Here the geometric area is dominated by the faces, which may have covalently-satisfied atomic planes in ideal form, but in most materials contain defects. The low edge/basal area ratio in ultrathin materials may result in basal defects driving much of the reactive surface chemistry.

An example of 2D material reactivity governed by basal defects is the $MoS_2$ oxidation study of Yamamoto et al.,[217] that uses AFM to track nucleation and growth of $O_2$ etch pits in large monolayer $MoS_2$ flakes on silica substrates. When organo-lithium intercalation is used for chemical exfoliation of TMDs, the resulting nanosheets are reported rich in internal edges (e.g. basal defects) due to the violent rupture process, and to possess high affinities for thiol groups shown by both experiment [218] and modeling.[219] As a result, chemically exfoliated $MoS_2$ can be easily functionalized with thiol-terminated ligands for applications.[218] Thiol-terminated polymers (e.g. lipoic acid modified PEG) can be grafted onto $MoS_2$ nanosheets through such thiol reactions to increase colloidal stability and biocompatibility for biomedical applications.[123]

Another behavior that is characteristic of layered materials is ion exchange to/from interlayer spaces. Layered double hydroxides, for instance, are anionic clays composed of trivalent cation substituted brucite-like layers with positive charges, compensated by exchangeable anions between layers. The high anion exchange capacity of LDHs has been utilized for the removal of anionic contaminants such as phosphate,[220] fluoride ions,[221] herbicide 2,4-dichlorophenoxyacetate.[222] The adsorption process is strongly dependent on the nature and content of di- and trivalent cations, and higher initial content of trivalent cations usually possess larger adsorption capacity.[220] Anionic molecules of larger size (*e.g.* sodium dodecylsulfate) can also be incorporated into LDH interspace via ion exchange.[223] Other clays such as montmorillonite and vermiculite have exchangeable interlayer *cations*,

and can be low-cost natural sorbents for heavy metal ion removal.[224–227] Vermiculite has been reported to adsorb heavy metal ions primarily at planar sites via cation exchange but also at layer edges through formation of complexes with oxygen-containing groups.[227]

Similar to cationic clays, titanate nanosheets[228] and vanadate based layered materials[229] consist of negatively charged layers and exchangeable interlayer cations. These nanomaterials have been reported to be applicable to the removal of toxic radioactive and heavy metal ions. Structural deformation of the thin layers has been observed induced by sorption of metal ions.[228, 229] Titanate nanosheets showed much more efficient ion exchange than other titanate materials and inorganic ion exchangers, which has been primarily attributed to the larger surface area of 2D nanosheets.[230] Larger cations like tetrabutylammonium can exchange with the cations and protons in the interlayer of layered titanate, which can induce osmotic hydration, expand the interlayer distance and ultimately lead to the exfoliation into single sheets.[231] The incorporation of guest molecules via cation exchange reaction into the interlayer of layered materials has been utilized to achieve the exfoliation of many other materials into the monolayer state.[232–236] $MnO_2$ nanosheets have negatively charges due to the presence of Mn(III) and vacant sites, and have been reported to adsorb Ni(II),[237] Uranium(VI),[238] Zn(II),[239], Co(II)[240] and others.[241] The adsorption of metal ions is sometimes followed by the oxidation of the adsorbed ions leading to the reductive dissolution of $MnO_2$.[239, 240] The reduction and environmental transformation of $MnO_2$ will be discussed in detail in a later section.

There have also been studies of macromolecular adsorption on 2D materials.[242, 243] The cationic biopolymer chitosan has been reported to intercalate in montmorillonite through cationic exchange[243] driven by electrostatic interactions between the $-NH^{3+}$ groups in the chitosan chain and the negatively charged planar sites. Poly(acrylic acid) can adsorb on the surface of $WS_2$ nanosheets by strong coordination of the carboxyl groups with tungsten atoms, imparting water-soluble $WS_2$ nanosheets.[242] $WS_2$ nanosheets can also be functionalized with bovine serum albumin through physical adsorption,[244] involving nonpolar amino acid residues and has been used in exfoliation methods to produce monolayer TMDs that are stable in aqueous suspension.[245]

Some 2D materials possess sufficient natural surface charge that they form stable colloids without molecular functionalization. TMD nanosheets prepared by organo-lithium intercalation and exfoliation, for example, have negative charges in the range of 0.15 – 0.25 electrons per metal atom[246] caused by electron transfer from the intercalant, promoting colloidal stability and affinity for cationic species.[247, 248] Overall, considering the enormous chemical diversity of 2D materials, much more work will be needed to achieve molecular-level understanding and control of the site-specific surface chemistry that mediates their biological and environmental behavior.

### 4.2 Physical and mechanical interactions - the biological response to 2D geometry

Two-dimensional materials are members of the larger class of high-aspect-ratio nanomaterials, whose 1D or 2D geometries lead to special physical and mechanical interactions with cells, microorganisms and tissues that in some cases produce pathological responses.[114–116, 254] Most of these data are for 1D materials (fibers and tubes), and the

limited 2D material data is for graphene-based materials. Because these are physical rather than chemical interactions, the data on graphene is relevant to our general understanding of the mechanical 2D–bio interface, and we will draw from that data significantly in this section. Figure 8 illustrates the modes of physico-mechanical interaction, which are governed by 2D geometry (thickness, lateral dimension, aspect ratio, shape), surface charge and polarity, and mechanical properties (bending stiffness, area extension modulus of cell membranes relative to the in-plane modulus of 2D materials). For graphene materials, the underlying mechanisms of cytotoxicity include plasma membrane damage,[114, 249, 255–259] impairment of mitochondrial activity,[258, 260] induction of oxidative stress,[174, 258, 260, 261] dissociation of proteins or peptides,[262, 263] and DNA/RNA damage,[264, 265] eventually leading to apoptotic and/or necrotic cell death,[266] as well as antimicrobial activities against a wide variety of microorganisms including bacteria,[249, 255, 259, 267–271] viruses,[272, 273] certain species of fungi,[268, 274, 275] algae,[276–279] protozoa,[280] and biofilm forming microorganisms.[267] Recently it has also been demonstrated that wrinkled graphene-based surfaces can dramatically direct cell alignment and morphology.[281] A key step to understanding these specific biological responses to 2D materials is to understand the modes of interaction between nanosheets and biomembranes, which strongly depend on 2D geometry, surface properties and mechanical properties.

Membrane interactions depend on material geometry, hydrophobicity, and the mechanical stiffness of the nanosheet relative to the lipid bilayer. Table 3 illustrates the range of mechanical properties expected for 2D materials and biomembranes with which they interact. The biomembrane thickness is 4–5 nm and a typical value of bending stiffness is on the order of 20 $k_B T$, where 1 $k_B T$=4.11×10$^{-21}$ J.[282] The bending stiffness of 2D nanosheets varies over a wide range and can be comparable to, or much larger than, the typical value of biomembrane, depending on the number of atomic layers and chemical composition (Table 3). Due to the high resistance to lateral stretching relative to bending, the 2D materials tend to deform primarily by bending during the interaction with biomembranes. Similarly, the biomembranes can be regarded as an inextensible elastic fluid membrane that also deforms primarily by bending. During the interaction, both the membranes and the 2D materials can undergo substantial configurational or structural transformation and mechanical deformation. The resulting interactive configuration is a delicate compromise among minimizing the mechanical deformation energy of the system, reducing contact between low affinity regions, and maximizing interactions between high affinity regions. On the basis of that compromise, one may find several different modes of interaction between 2D materials and biomembranes, depending strongly on the geometry (size, shape), surface properties and elasticity of 2D materials (Fig. 8).

**4.2.1 Local disturbance of biomembranes by 2D materials—**Recent experiments and molecular dynamics simulations demonstrate that pristine graphene and graphene oxide (GO) sheets can pierce into and extract lipid molecules from *Escherichia coli* lipid membranes (Fig. 8a), inducing loss of membrane integrity.[249, 259] If their lateral sizes are comparable to the lipid membrane thickness, pristine or lightly functionalized graphene nanoflakes can either align parallel at the interface between the two lipid monolayers (Fig. 8b) or cut across the membrane as a transmembrane object (Fig. 8c).[250, 251, 283, 284] Further

investigations with molecular dynamics simulations showed that graphene nanoflakes with 5% of their edge carbon atoms functionalized with hydrophilic oxygen-containing groups stay parallel between the two lipid leaflets (monolayers), while those with 10% oxidized edge atoms adopt a near-perpendicular transmembrane configuration.[251] Similar configurations have also been observed for few-layer-graphene and graphene oxide nanostructures.[250, 251] For 5% or less edge oxidization, the energetically favorable interaction between hydrophobic regions of the embedded oxidized graphene nanoflake and hydrophobic lipid hydrocarbon chains is proportional to the large contact area in the parallel embedded configuration and overcomes the energetically unfavorable exposure of the lightly hydrophilic edges to hydrophobic lipid hydrocarbon chains. Therefore, the parallel embedding configuration becomes a stable state, similar to the case of pristine graphene flakes.[250] As the edges become highly oxidized (*e.g.* 10% or more edge atoms oxidized), the energetically unfavorable exposure of the oxidized edge atoms to lipid hydrocarbon chains prevails over the nonpolar interaction in the parallel configuration, and a near-perpendicular transmembrane configuration becomes energetically favorable with the oxidized edge atoms exposed to the polar lipid head groups and water.

Meanwhile, graphene microsheets can spontaneously pierce into a lipid bilayer membrane at corners (Fig. 8d) or edge asperities (Fig. 8e). For corner piercing, there exists only a small energy barrier, comparable to the thermal energy $k_B T$, while a high barrier exists for smooth edge contact in the absence of a sharp corner.[114] A recent theoretical analysis indicated that transmembrane 2D materials adopt a near-perpendicular configuration with respect to the cell membrane, driven by the splay and membrane tension energies.[285] The reorientation of 2D materials between the near-perpendicular transmembrane and parallel-embedded configurations is subject to an energy barrier arising from the motion and deformation of lipid molecules, which is proportional to the size of the 2D material. For micro-sized 2D materials, the energy barrier is too large to be overcome by thermal fluctuation. Therefore, 2D graphene sheets, of micron-scale lateral dimension (microsheets), after spontaneous perpendicular piercing at edge asperities or corner sites, would adopt a near-perpendicular transmembrane configuration instead of parallel embedding in the lipid bilayer as small nanoflakes do.[114, 250]

Experimental studies have shown that the interaction between graphene-family 2D materials and bacteria, viruses as well as fungi could lead to strong antibacterial,[267–270, 276] antiviral[272, 273] and antifungal[268, 274, 275] activities. For example, the antibacterial activity of graphene and GO sheets might be attributed to damage on bacterial membranes induced by the atomically sharp edges of the 2D sheets as demonstrated in Fig. 8a–e. Such physical damage could lead to loss of membrane integrity,[249, 255, 270] leakage of RNA, and changes in the transmembrane potential.[268] Furthermore, not only the membrane stress arising from membrane damage but also oxidative stress can contribute to the antibacterial activity.[270] A size-dependent antimicrobial activity of GO has also been revealed recently.[269, 271] Regarding the antiviral activity, GO and sulfonated rGO could block the infection of herpes simplex virus type 1 through cell attachment inhibition at low concentrations.[272] GO sheets exhibit antiviral activity against pseudorabies virus and porcine epidemic diarrhea virus prior to their viral entry.[273] rGO sheets could completely inhibit the mycelial growth of the fungi *Aspergillus niger, Aspergillus oryzae* and *Fusarium oxysporum* at the concentration of 500

μg/ml, 500 μg/ml, and 250 μg/ml, respectively.[274] Similar antifungal activity of GO and rGO against pathogenic fungi *Fusarium graminearum* and *Fusarium poae* has also been reported.[268, 275] Further studies on the interaction between 2D materials of different kind, size, shape and functionality and different type of cells and microorganism will be needed in order to gain a more general understanding of the cytotoxicity mechanism of 2D materials in general.

**4.2.2 Cell adhesion and internalization of 2D materials—**Cellular internalization following initial adhesion is of fundamental importance for uptake of nutrients and signaling molecules. Recent studies indicate that internalization of 2D materials is substantially influenced by their size, as in the cellular uptake of nanoparticles. For example, large (1 μm lateral dimension) protein-coated GO sheets, following initial attachment to the membranes of fish liver cells (PLHC-1) (Fig. 8f), enter cells predominantly through phagocytosis; while small protein-coated GO sheets are internalized through clathrin-mediated endocytosis.[252] Large GO sheets can form wrinkled structures due to the strong adhesion with cell membranes (Fig. 8g).[253] Although GO with lateral sizes of 350 nm and 2 μm exhibit similar accumulation in peritoneal macrophages after 24 hours incubation, detailed analysis on uptake pathways shows that the 350 nm GO sheets are wrapped by the active filopodia of macrophages while some 2 μm GO sheets undergo an near-perpendicular entry with respect to the cell membrane. Compared to the 350 nm GO sheets which remain in their initial shapes, the 2 μm GO form wrinkles and tend to fold into lysosomes (Fig. 8h),[174] which demonstrates the importance of mechanical flexibility in these atomically thin 2D materials. Since the wrinkles could modify the electrical conductivity of graphene, this approach may also be used to sense and measure cellular responses such as variation of cell volume and membrane tension.[309, 310] It is observed that human THP-1 macrophages exposed to few-layer graphene sheets with lateral size up to 5 μm can readily internalize the latter, while macrophages exposed to 25 μm few-layered graphene sheets could only adhere to and spread on the graphene surface (Fig. 8i and j).[19] Similar size-dependent interaction behaviors are also observed as *E. coli* cells are exposed to GO of different sizes, where large GO sheets with average area of 13 $\mu m^2$ can fully cover and isolate the bacteria, and consequently prohibit the proliferation of bacteria (Fig. 8k); while small GO sheets (0.2 $\mu m^2$) stick to the *E. coli* cell membrane but have no effect on bacteria proliferation and viability.[118] Other studies demonstrate that the full coverage and isolation induced by attaching 2D materials such as calcium phosphate layers on yeast cells can enhance cell viability and protect cells by reducing biological communication with the environment.[311] Similar protective encapsulation of living yeast cells with GO sheets has also been reported.[310, 312] The central panel in Fig. 8 is a schematic representation of the above interaction modes (a-k) as well as endocytic uptake (l) which has been demonstrated to be specific to the size of the internalized 2D materials.[252]

Studies on the interaction between graphene-family materials and microorganisms in aquatic ecosystems such as algae and protozoa are relatively rare.[276–280] It has been reported that the entrapment of *Chlorella vulgaris* microalgae with GO layers can effectively suppress the rate of cell division.[279] Recent experiments indicate that GO sheets of lateral size 120–200 nm cause a growth inhibition up to 50% of the green algae *Raphidocelis subcapitata* at a GO

concentration of 20 μg/ml, and there is a positive correlation between oxidative stress and membrane damage as the GO concentration is higher than 10 μg/ml. Agglomeration of GO sheets might also result in shading and thus reduce the exposure of algae to light and depression of algal photosynthesis.[277] The adverse effects of GO sheets against the viability of algal cells have also been observed in the case of the algae *Chlorella vulgaris*, where GO sheets enter the cells, damage organelles, induce excess generation of reactive oxygen species and eventually inhibit cell growth.[276] Similar ecotoxicological effects of GO on the protozoa *Euglena gracilis* have also been reported recently.[280]

As demonstrated in Fig. 8h, Fig. 2D materials may be fully packaged into subcellular vesicles following uptake. In this case, the encapsulating subcellular vesicle would undergo elastic deformation if the lateral size of the internalized 2D material is larger than the diameter of the vesicle. Since the length scale of membrane deformation is typically much larger than membrane thickness, the vesicle can be simply modeled as a closed inextensible surface with bending stiffness $\kappa$.[313] For a vesicle of effective radius $a$ and surface area $A_t=4\pi a^2$ containing a two-dimensional circular sheet of diameter $L(\geq 2a)$, the elastic energy $E_{el}$ and shape of the deformed vesicle can be determined through the variational of the Canham-Helfrich functional.[313–316] With the knowledge of $E_{el}$, the compressive interaction force per unit contact length between the vesicle and the packaged 2D material is simply $f=dE_{el}/d[\pi(L/2)^2]$.

Fig. 9a shows the compressive contact force per unit length $f$ between the vesicle membrane and the encapsulated 2D material at zero osmotic pressure. The bilayer membrane is composed of two chemically identical monolayers, with zero spontaneous curvature. As the length ratio $L/(2a)$ increases, the contact force per unit length $f$ increases (Fig. 9a). The critical buckling force per unit length of the packaged 2D material is $f_c=16.79\kappa_p/L^2$, where $\kappa_p$ is its bending stiffness.[317] Substituting $f_c$ into $f$, we can draw a simple buckling phase diagram with respect to the length ratio $L/(2a)$ and bending stiffness ratio $\kappa_p/\kappa$ between the internalized 2D material and the encapsulating vesicle. As indicated in Fig. 9b, the larger and softer the encapsulated 2D material is, the easier it buckles. Typical bending stiffnesses of some 2D materials are listed in Table 3. A combination of Fig. 9b and Table 3 indicates the regimes in which the corresponding 2D materials would buckle. For subcellular vesicles such as endosomes and lysosomes, typical parameters are $a$=0.5 μm, $\kappa$=20 $k_BT$, and the lysis membrane tension is on the order of $\sigma_s$=1 pN/nm.[306] These typical values correspond to a length ratio $L/(2a)\approx 1.4$ and a bending stiffness ratio $\kappa_p/\kappa\approx 2800$, defining the regime in which the encapsulated 2D material could lyse the cell membrane. This result suggests that some 2D materials ($\kappa_p/\kappa \leq 40$) listed in Table 3 could indeed buckle under the compressive contact force induced by the membrane unless other damage mechanisms such as corner penetration or lipid extraction occur.

More research is clearly needed to understand the fundamental interactions of biological systems with 2D nanosheets, including studies of membrane penetration, lipid extraction, cellular uptake, and intracellular vesicular packaging and lysosomal damage mechanisms. These physico-mechanical effects are relevant to all types of 2D materials, and we hope that fundamental studies will reveal the general principles behind these behaviors and their

relation to basic material properties such as thickness, lateral dimension, mechanical stiffness and hydrophobicity/−philicity.

### 4.3. Electronic and Surface Redox Interactions

Oxidation/reduction reactions at solid material surfaces have long been recognized as important initiators of adverse biological responses either to ambient fine particulate matter or to engineered nanomaterials.[318] Solid surfaces may interact directly with biological target molecules, or interact indirectly through reaction with $H_2O_2$ or dissolved $O_2$ producing reactive oxygen species (ROS) that subsequently damage proteins, nucleic acids, or lipids. At sufficient particle dose, these reactions may induce oxidative stress – a pathological state of cellular imbalance between oxidant products and the cell's antioxidant defenses. Redox reactions involve electron or H• transfer to/from solid surfaces and often occur in a catalytic cycle, which for biopersistent particles can show sustained activity. Being solid-fluid interface reactions, this form of biological activity is typically enhanced by high material surface area and is thus potentially quite significant for monolayer and few-layer 2D materials. Also, being surface reactions, these are complex processes that depend not only on material structure and phase, but also redox-active surface states (*e.g.* quinone groups, bound Fe) that depend on processing history, impurities, coatings or adsorbates.

Some 2D materials are well-known catalysts in non-biological settings (*e.g.* $MoS_2$, $MnO_2$, $TiO_2$)[319–321] but little is known about their biological redox activity. At this early stage in the 2D material field, there is strong motivation to develop classification schemes for screening materials to set priorities for experimental research, or as part of tiered toxicity testing strategies. Many 2D materials are semiconductors, whose electron transfer characteristics may be expected to depend on allowed and disallowed energy levels in their band structures. A classification system has recently been proposed for semiconductor nanoparticles based on the overlap between conduction band edges (that contain allowed, unoccupied states) and electron energy levels associated with biological redox couples.[192, 322, 323] The hypothesis is that when these two energy levels overlap, electron transfer events are energetically permissible in both directions, and could perturb normal biological redox pathways in a manner that ultimately induces adverse responses. Plumlee *et al.*[323] use a set of important biological redox couples that together define a band referred to as the cellular redox potential, whose energy levels have been compared to nanomaterial conduction band edges, leading to some early correlative ability with observed redox activity.[192]

Figure 10 shows published data on band energies for a selection of layered and reference materials and their positions relative to the cellular redox potential. The comparison suggests the potential for biological redox activity in graphene, $MoS_2$, $MnO_2$ nanosheets, and single-walled carbon nanotubes (SWCNTs) based on overlap of the conduction band edge and cellular redox potential. Biological redox activity has indeed been reported for graphene and SWCNTs,[258, 324, 325] and experimental study of $MoS_2$ and $MnO_2$ are a priority for new research. A clearly contrasting case is h-BN, which does not have allowed electron energy levels overlapping with or even near to the cellular redox potential. An interesting feature of Fig. 10c is the existence of a set of materials whose *valence band* overlaps with the cellular

redox potential or the ROS-involved redox couples. Because catalytic redox processes involve electron transfer both to and from allowed states, the populated states at the top of the valence band may also initiate activity through electron donation to biomolecular redox couples accompanied by hole formation and refilling in a catalytic cycle. Experimental research is needed to verify if this subset of materials does indeed show biological redox activity, and whether valence-band alignment is a useful criterion for screening 2D materials. An important caveat in this analysis is that some band energies used here are those of bulk crystals, while band structures of actual 2D materials will be affected by other factors such as doping, exfoliation (thickness dependence), and compressive strain.[326–330]

Overall, this review suggests that surface redox reactions will be important for many 2D materials due to their ultrahigh surface area and wide range of electronic band structures. Research is needed to characterize this redox activity as function of material composition and phase, specific edge states and functionalization, doping, intercalation, adsorption, as well as a critical evaluation of new quantitative structure-activity relations (QSAR) approaches for semiconducting forms based on electronic band structure. A particular focus is recommended on materials that are stable to dissolution (Section 4.1), which through their biopersistence may exert solid-state redox activity over long time periods.

## 5. Chemical transformations in the natural environment

A comprehensive understanding of the environmental implications of 2D materials will require knowledge of their releases, transport through environmental media, partitioning, chemical and physical transformations, bioaccumulation, and effects on environmental organisms and ecosystems.[27, 110, 112, 124, 215, 326, 339] Here we focus on chemical transformations with the goal of identifying the material forms that will play the most important roles in the natural environment. This issue is informed by a decade of research on the environmental implications of particulate and 1D nanomaterials[340, 341] plus significant data on the environmental chemistry of natural 2D materials.[342–348]

### 5.1 Chalcogenides

Metal chalcogenides are often regarded as relatively stable under ambient conditions,[22] but careful review of the broader literature reveals their ability to undergo environmental transformation. While many metal sulfides have very low solubilities,[177] they are susceptible to environmental oxidation, as the thermodynamic analysis in Section 4.1 shows, and in most cases that oxidation leads to soluble products. Recent work on few-layer $MoS_2$ confirms dissolution over time scale of days in laboratory experiments using environmental and biological simulant fluids.[213] Zhang *et al.*[125] also found that $Bi_2Se_3$ was oxidized easily in air, and in biodistribution studies using a mouse model, report *in vivo* oxidation of $Bi_2Se_3$ accompanied by release of free Se species. Single- and few-layer $MoS_2$ has been found to undergo photo-induced corrosion process, where the edge sites and presumably also defect sites are the primary degradation targets (Fig. 11 a–d), converting $MoS_2$ into soluble $MoO_x$ that dissolves in the electrolyte.[214] The photodegradation of $MoS_2$ depends on the presence of oxygen in the electrolyte, evidenced by significantly reduced degradation rate monitored by $MoS_2$ Raman intensity when reduced oxygen concentration was used (Fig. 11e).

Also relevant are biogeochemical studies that demonstrate metal sulfide oxidation processes mediated by bacteria. “Bacterial leaching” is a term used in the geochemistry literature for biooxidation to soluble metal and sulfur species (*e.g.* sulfate) by bacterial specialists such as *Thiobacillus ferrooxidans, Leptospirillum ferrooxidans* and *Thiobacillus thiooxidans*.[349] In direct leaching, physical contact between bacteria and sulfide mineral surfaces is required, and oxidation occurs through multiple steps catalyzed by enzymes. In indirect bioleaching, the biooxidation of sulfide minerals is mediated by ferric iron generated by bacteria. Here the bacteria act essentially as a catalyst for re-oxidation of ferrous iron, which otherwise takes place very slowly. The products of molybdenite ($MoS_2$) oxidation have been reported to be sulfuric acid and molybdic acid ($H_2MoO_4$).[350] Faster oxidation leaching of molybdenite was observed in the molybdenite sample with smaller particle size,[350] which highlights the need for experimental studies of oxidative leaching of molybdenite in its 2D form. The indirect biooxidation of molybdenite can occur through a mechanism where thiosulfate is first produced and then oxidized by ferric iron in a series of reactions generating tetrathionate ($S_4O_6^{2-}$), disulfane-monosulfonic acid ($HSSSO_3^-$) and finally sulfate ($SO_4^{2-}$).[351] $WS_2$ has been reported to behave similarly as $MoS_2$ in terms of environmental stability and bio-oxidation.[352] Beyond oxidative dissolution, other phase changes in TMDs are conversion from the semiconducting 2H phase to the metallic 1T form induced by alkali metal intercalation.[188]

Metal phosphorus trichalcogenides (listed as thiophosphates and selenophosphates in Table 1), possess interesting magnetic and ferroelectric properties as well as suitable band gaps for visible-light driven applications (*e.g.* water splitting),[353] which suggests they may undergo photo-induced degradation or transformation in the environment. Similar to layered TMDs, these layered metal phosphorus trichalcogenides can undergo intercalation reactions[354–356] including cationic substitution-intercalation reactions, where a cation from the environment can replace and remove the original cation in the host lattice, leading to release of potential toxic ions such as Cu, Cd, Ni, or Co.[355, 357–359]

### 5.2 Oxides

In the natural environment, metal oxides may undergo simple (non-redox) dissolution or reductive dissolution depending on their chemistry and the local fluid composition. The equilibrium solubility of 2D oxide materials varies greatly, as seen in Fig. 7b. Most of these 2D oxides have solubilities > $10^{-4}$ M, which is sufficient to cause complete dissolution at the low material concentrations (mg/L) relevant to environmental release scenarios. Dissolution of layered double hydroxides nanoparticles has been observed[360] and has been studied in detail in the context of mineral weathering.[361] The dissolution process is known to be complex, involving mass transport, adsorption, interlattice migration, reaction, and desorption, and to depend on acidity, reactive species concentration and ligand concentrations.[361]

Reductive dissolution is also an important environmental pathway for some 2D oxide materials. For example, $MoO_3$ in organic soil extracts has been shown to undergo reduction from the +6 oxidation state to Mo(V) or Mo(III) in the presence of humic acids.[362] Vanadium pentoxide ($V_2O_5$) becomes more soluble upon reduction, which can be explained

by the greater lability of reduced metal-oxygen bond.[361] In general, reductive dissolution of oxide minerals is one of the most important transformations in the geochemical cycling of electrons.[361]

There is significant data on the reductive dissolution of manganese oxides. $MnO_6$ octahedra are the basic building units for Mn(IV) oxides, and are assembled by sharing edges and/or corners to construct tunnel structures and layer structures.[347] More than 30 natural and synthetic Mn oxides have been characterized, and such diversity is attributed to various environmentally stable oxidation states of Mn and many potential arrangements of octahedra units.[347] In environmental settings, Mn oxides readily undergo cation exchange reactions with a preference for Ni, Co and Ba over Ca and Mg,[363, 364] and this property has been employed in the adsorptive removal of heavy metal pollutants such as Pb, Cu, Zn and Cd.[343, 345, 346, 365] Based on thermodynamics, manganese should exist in oxic waters as insoluble $MnO_2$, however, most of the manganese in near-surface water exists as soluble species Mn(II).[366] The maintenance of lower oxidation state of Mn has been attributed to slow oxidation kinetics of Mn(II) and the presence of reductants in the environment that convert $MnO_2$ to soluble Mn(II).[348] Manganese oxides have been shown to undergo reduction with release of soluble Mn(II) in the presence of a variety of environmental reductants, including reduced metal ions,[363] natural organic matter (NOM),[348, 367] and organic contaminants.[347, 368] Generally, the reduction of $MnO_2$ is a surface-controlled process[368] and the specific surface area of manganese oxides shows positive correlation with its reduction and dissolution rate,[369] suggesting that monolayer and few-layer forms will undergo rapid reduction and dissolution. The reduction rate of $MnO_2$ is strongly pH-dependent,[368] and accelerated by solar irradiation in the presence of by dissolved NOM in aqueous environments.[342, 348] A recent review is available on the reductive transformation of $MnO_2$ in the presence of organic pollutants.[347] In the absence of organic electron donors, $MnO_2$ nanosheets were observed undergo photo-reduction under environmental-relevant conditions involving formation and migration of interlayer Mn(III) ions, which are stabilized by adsorption at interlayer sites and increase nanosheet stacking (Fig. 11e).[370]

While many chalcogenides and oxides are anticipated to undergo environmental transformation, other emerging 2D materials are likely persistent. Boron nitride for example is considered stable in bulk form with good resistance to air oxidation and moisture hydrolysis.[344] Ultrathin exfoliated h-BN films have also been applied as coatings that withstand extreme environments.[371] For many of the other emerging 2D materials (Fig. 1), there are no data on environmental transformation, and this is clearly an important area for further research.

## 6. Conclusions and recommendations

The biological and environmental interactions of 2D materials is an important new research field, whose results will enable biomedical and environment technologies, and will inform the process of human health risk assessment and safe material design and development for all 2D material applications. This review combines recent data on monolayer and few-layer forms with older literature on the environmental and health effects of bulk layered materials

to identify the essential chemical behaviors and suggest high-priority topics for future research.

The biological response to 2D materials varies greatly, as expected from their chemical diversity, with studies reporting low toxicity for some materials (*e.g.* $MoS_2$, h-BN) and more significant effects for others (*e.g.* vanadium and manganese oxides, some selenides, tellurides). The extreme diversity of 2D materials in both chemistry and physical form provide many opportunities for chemical researchers, but also poses a challenge for any comprehensive assessment of health effects. This review therefore proposes a framework for seeking a more systematic understanding of biological effects based on fundamental materials chemistry and physics. The framework considers three fundamental interaction modes: chemical, electronic, and physico-mechanical.

In the area of chemical interactions, thermodynamic analysis and biogeochemical data show that many layered materials can undergo dissolution in biological systems or the natural environment. Because dissolution has profound effects on overall behavior, there is an urgent need for much more experimental dissolution data on specific 2D monolayer and few-layer forms, covering kinetics, pH, salt, and ligand effects in complex media. For many 2D materials, dissolution occurs with change of oxidation state, and must be understood as a chemical reaction with local oxidizing or reducing agents to liberate soluble products and/or transformed solid phases. Oxidative dissolution is a well-known phenomenon for particulate (non-2D) nanomaterials (*e.g.* Ag, Cu, CdSe). In contrast, reductive dissolution has been largely overlooked in the nanotoxicology literature, but appears to be important for some 2D materials such as $MnO_2$ and $MoO_3$. For all dissolving systems, their biological effects are best interpreted and understood in terms of the chemical toxicity of the soluble transformation products mediated by the timing and location of their release from the nanosheet phase. Here a reasonable path to risk assessment is to better characterize dissolution (kinetics, product distributions), and to couple this information with existing data on the biological effects of the relevant soluble species. This two-part strategy offers a rationale route to interpreting cell culture or *in vivo* data and carrying out hazard assessments for this class of materials.

Other 2D materials are likely to be persistent in the environment and/or in living systems. Such materials may pose a special risk of long-latency disease development, based on our experience with human exposure to other materials such as sheet-like silicates (see case study in Section 3.3). Longer-term biopersistence can be difficult to study in the laboratory, but its importance provides ample justification for such studies on emerging 2D materials. For persistent materials, the goal of understanding the materials basis for biological responses focuses attention on electronic (surface redox) and physico-mechanical interaction modes.

Physical and mechanical interactions play a special role for emerging 2D materials, which belong to the larger class of high-aspect-ratio nanomaterials. Some of these materials are known to initiate adverse biological responses through membrane penetration and damage, frustrated phagocytosis and impaired lung clearance, and lysosomal damage. These geometry/shape-dependent effects are common to all 2D material chemistries, and define a

new subfield interested in atomically thin sheet structures interacting with membranes and subcellular organelles. There is a particular need to understand how large lateral dimension (>1μm) sheets interact with cells and tissue, as early research on graphene has identified this material subset as potentially hazardous. Most work to date on 2D materials "beyond graphene" has used small-lateral-dimension sheets (typically < 300nm), and of course these results do not provide any information on large-sheet behavior. Application demands will likely drive the 2D synthesis field toward larger primary sheet dimension, and as these synthesis methods improve, we can expect to see unique large-sheet effects in the biological response, as suggested by the early graphene literature. Another fertile research area is the role of stiffness, as some near-atomically-thin sheets may be "biologically soft" (i.e. deformable by soft cellular forces) and thus not perceived by cells as rigid plates with implications for uptake, intracellular packaging and frustration.

The final interaction mode involves electronic and surface redox processes, which will also be especially important for the subclass of persistent (non-dissolving) 2D materials. In this area, the field needs direct experimental data on redox activity in both simple and complex media, as well as an assessment of new screening concepts based on band structure analysis. An open question is the extent to which bulk electronic properties will be useful predictors, and the extent to which special surface states, exfoliation degree, intercalation effects, or other effects will govern redox activity in biological environments.

Overall, a list of the highest priority research topics in this new area include: (i) release and exposure studies for the major classes of synthesis methods, (ii) dissolution and phase transformation studies in complex media, (iii) *in vitro* studies of cellular response to nanosheets of diverse chemistry and physical form, (iv) longer-term measurements of degradation and biopersistence, (v) simulation of and experiments on nanosheet physico-mechanical interaction with cellular substructures, especially to sheets with large (supramicron) lateral dimension, (vi) consideration of chemical hazards and processing safety associated with nanosheet precursors and byproducts, and (vii) development of screening tools and generalized analytical or in silico methods to predict redox activity, dissolution, transformation for the broad class of 2D materials, and (vii) ultimately, *in vivo* studies addressing phagocytosis, lung clearance, translocation, biopersistence, inflammatory activity potentially modified by surface adsorption *in vivo* based on experience with human exposure to natural materials including sheet-like silicates.

It is clear that the "bio-nanosheet interface" is an exciting new area that will offer many opportunities for novel scientific research over the next decade. While this research is underway, it is also clear that R&D activities on synthesis, fabrication, and application of emerging 2D nanomaterials should be conducted in a manner that limits exposure, as a precautionary measure, using proper engineering controls and sound laboratory and workplace practices, until the many scientific issues raised in this review are better resolved.

## Supplementary Material

Refer to Web version on PubMed Central for supplementary material.

## Acknowledgments

Financial support for this work was provided by the Superfund Research Program of the National Institute of Environmental Health Sciences (Superfund Research Grant 2P42 ES013660-1), Office of Naval Research (Grant N00014-15-1-2452) and the National Science Foundation (Grant INSPIRE Track 1 CBET-1344097).

## References

1. Geim AK, Novoselov KS. Nat. Mater. 2007; 6:183–191. [PubMed: 17330084]
2. Novoselov KS, Geim AK, Morozov S, Jiang D, Zhang Y, Dubonos S, Grigorieva I, Firsov A. Science. 2004; 306:666–669. [PubMed: 15499015]
3. Lembke D, Kis A. ACS Nano. 2012; 6:10070–10075. [PubMed: 23039374]
4. Eda G, Yamaguchi H, Voiry D, Fujita T, Chen M, Chhowalla M. Nano Lett. 2011; 11:5111–5116. [PubMed: 22035145]
5. Dresselhaus, M., Dresselhaus, G. Intercalation in Layered Materials. Plenum, New York: NATO Advanced Study Institute, Series B; 1986.
6. Shrimpton, N., Cole, M., Steele, W., Chan, M., Benedek, G. Surface Properties of Layered Structures. Boston, MA: Kluwer; 1992.
7. Lieth, R. Preparation and crystal growth of materials with layered structures. Springer Science & Business Media; 1977.
8. Levy, F. Physics and Chemistry of Materials with Layered Structures. Vol. 2. D. Reidel Publishing Co; 1976.
9. Lee, PA. Optical and electrical properties. Springer Science & Business Media; 2012.
10. Grasso, V. Electronic structure and electronic transitions in layered materials. Springer Science & Business Media; 1986.
11. Hulliger, F. Structural Chemistry of Layer-Type Phases. Dordrecht: D. Reidel Publishing Company; 1976.
12. Fong, C., Schlüter, M. Electrons and phonons in layered crystal structures. Wieting, TJ.Schlüter, M., Reidel, Dordrecht, editors. 1979. p. 145
13. Besenhard J, Müller-Warmuth W, Schöllhorn R. Progress in Intercalation Research. 1994:457–508.
14. Daage M, Chianelli R. J. Catal. 1994; 149:414–427.
15. Nicolosi V, Chhowalla M, Kanatzidis MG, Strano MS, Coleman JN. Science. 2013; 340:1226419.
16. Chen Y, Tan C, Zhang H, Wang L. Chem. Soc. Rev. 2015; 44:2681–2701. [PubMed: 25519856]
17. Perreault F, de Faria AF, Elimelech M. Chem. Soc. Rev. 2015; 44:5861–5896. [PubMed: 25812036]
18. Zhao J, Wang Z, White JC, Xing B. Environ. Sci. Technol. 2014; 48:9995–10009. [PubMed: 25122195]
19. Sanchez VC, Jachak A, Hurt RH, Kane AB. Chem. Res. Toxicol. 2011; 25:15–34. [PubMed: 21954945]
20. Mao HY, Laurent S, Chen W, Akhavan O, Imani M, Ashkarran AA, Mahmoudi M. Chem. Rev. 2013; 113:3407–3424. [PubMed: 23452512]
21. Wiesner MR, Lowry GV, Alvarez P, Dionysiou D, Biswas P. Environ. Sci. Technol. 2006; 40:4336–4345. [PubMed: 16903268]
22. Chhowalla M, Shin HS, Eda G, Li LJ, Loh KP, Zhang H. Nat Chem. 2013; 5:263–275. [PubMed: 23511414]
23. Miró P, Audiffred M, Heine T. Chem. Soc. Rev. 2014; 43:6537–6554. [PubMed: 24825454]
24. Wang QH, Kalantar-Zadeh K, Kis A, Coleman JN, Strano MS. Nat. Nano. 2012; 7:699–712.
25. Mas-Balleste R, Gomez-Navarro C, Gomez-Herrero J, Zamora F. Nanoscale. 2011; 3:20–30. [PubMed: 20844797]
26. Zhan Y, Liu Z, Najmaei S, Ajayan PM, Lou J. Small. 2012; 8:966–971. [PubMed: 22334392]
27. Han JH, Lee S, Cheon J. Chem. Soc. Rev. 2013; 42:2581–2591. [PubMed: 23212120]
28. Miró P, Han JH, Cheon J, Heine T. Angew. Chem. Int. Ed. 2014; 53:12624–12628.

29. Bianco E, Butler S, Jiang S, Restrepo OD, Windl W, Goldberger JE. ACS Nano. 2013; 7:4414–4421. [PubMed: 23506286]
30. Kong D, Koski KJ, Cha JJ, Hong SS, Cui Y. Nano Lett. 2013; 13:632–636. [PubMed: 23323715]
31. Li J, Chen Z, Wang R-J, Proserpio DM. Coord. Chem. Rev. 1999; 190:707–735.
32. Wang M, Koski KJ. ACS Nano. 2015; 9:3226–3233. [PubMed: 25734624]
33. Keuleyan S, Wang M, Chung FR, Commons J, Koski KJ. Nano Lett. 2015; 15:2285–2290. [PubMed: 25764295]
34. Murugan AV, Muraliganth T, Manthiram A. Chem. Mater. 2009; 21:5004–5006.
35. Wang W, Poudel B, Yang J, Wang D, Ren Z. J. Am. Chem. Soc. 2005; 127:13792–13793. [PubMed: 16201791]
36. Zhou B, Ji Y, Yang Y-F, Li X-H, Zhu J-J. Cryst. Growth Des. 2008; 8:4394–4397.
37. Vaughn Ii DD, Patel RJ, Hickner MA, Schaak RE. J. Am. Chem. Soc. 2010; 132:15170–15172. [PubMed: 20942394]
38. Yoo D, Kim M, Jeong S, Han J, Cheon J. J. Am. Chem. Soc. 2014; 136:14670–14673. [PubMed: 25313652]
39. Zhi C, Bando Y, Tang C, Kuwahara H, Golberg D. Adv. Mater. 2009; 21:2889–2893.
40. Cai G, Jian J, Chen X, Lei M, Wang W. Appl. Phys. A. 2007; 89:783–788.
41. Frindt RF. J. Appl. Phys. 1966; 37:1928–1929.
42. Tatlock G, Acrivos JV. Philos. Mag. B. 1978; 38:81–93.
43. Blackwelder E. J. Geol. 1925:793–806.
44. Woltornist SJ, Oyer AJ, Carrillo J-MY, Dobrynin AV, Adamson DH. ACS Nano. 2013; 7:7062–7066. [PubMed: 23879536]
45. Coleman JN, Lotya M, O'Neill A, Bergin SD, King PJ, Khan U, Young K, Gaucher A, De S, Smith RJ. Science. 2011; 331:568–571. [PubMed: 21292974]
46. Smith RJ, King PJ, Lotya M, Wirtz C, Khan U, De S, O'Neill A, Duesberg GS, Grunlan JC, Moriarty G. Adv. Mater. 2011; 23:3944–3948. [PubMed: 21796689]
47. Li H, Lu G, Wang Y, Yin Z, Cong C, He Q, Wang L, Ding F, Yu T, Zhang H. Small. 2013; 9:1974–1981. [PubMed: 23281258]
48. Magda GZ, Pető J, Dobrik G, Hwang C, Biró LP, Tapasztó L. Sci. Rep. 2015:5.
49. Paton KR, Varrla E, Backes C, Smith RJ, Khan U, O'Neill A, Boland C, Lotya M, Istrate OM, King P. Nat. Mater. 2014; 13:624–630. [PubMed: 24747780]
50. Yu X, Prévot MS, Sivula K. Chem. Mater. 2014; 26:5892–5899.
51. Fukushima Y, Okada A, Kawasumi M, Kurauchi T, Kamigaito O. Clay Miner. 1988; 23:27–34.
52. Zeng Z, Yin Z, Huang X, Li H, He Q, Lu G, Boey F, Zhang H. Angew. Chem. Int. Ed. 2011; 50:11093–11097.
53. Auerbach, SM., Carrado, KA., Dutta, PK. Handbook of layered materials. CRC Press; 2004.
54. Dines MB. Mater. Res. Bull. 1975; 10:287–291.
55. Benavente E, Santa Ana M, Mendizábal F, González G. Coord. Chem. Rev. 2002; 224:87–109.
56. Golub AS, Zubavichus YV, Slovokhotov YL, Novikov YN. Russ. Chem. Rev. 2003; 72:123–141.
57. Py M, Haering R. Can. J. Phys. 1983; 61:76–84.
58. Hull, M., Bowman, D. Nanotechnology Environmental Health and Safety: Risks, Regulation, and Management. William Andrew; 2014.
59. Schinwald A, Murphy FA, Jones A, MacNee W, Donaldson K. ACS Nano. 2012; 6:736–746. [PubMed: 22195731]
60. Pauluhn J. Toxicol. Sci. 2009:kfp247.
61. Bosi M. RSC Adv. 2015; 5:75500–75518.
62. Nandi DK, Sen UK, Choudhury D, Mitra S, Sarkar SK. Electrochim. Acta. 2014; 146:706–713.
63. Cheon J, Gozum JE, Girolami GS. Chem. Mater. 1997; 9:1847–1853.
64. Plata DL, Hart AJ, Reddy CM, Gschwend PM. Environ. Sci. Technol. 2009; 43:8367–8373. [PubMed: 19924971]
65. Moxon AL, Rhian M. Physiol. Rev. 1943:23.

66. James L, Mayland H, Panter K. Rangelands. 1991; 6:64–67.
67. Shie MD, Deeds FE. Public Health Reports (1896–1970). 1920:939–954.
68. Garro F, Pentschew A. Archiv für Psychiatrie und Nervenkrankheiten. 1964; 206:272–280. [PubMed: 14344121]
69. Chasteen TG, Bentley R. Chem. Rev. 2003; 103:1–26. [PubMed: 12517179]
70. Moroder L. J. Pept. Sci. 2005; 11:187–214. [PubMed: 15782428]
71. Nogueira CW, Zeni G, Rocha JB. Chem. Rev. 2004; 104:6255–6286. [PubMed: 15584701]
72. Gray N. Environ. Geol. 1997; 30:62–71.
73. Simate GS, Ndlovu S. Journal of Environmental Chemical Engineering. 2014; 2:1785–1803.
74. Javaherdashti, R., Nwaoha, C., Tan, H. Corrosion and materials in the oil and gas industries. CRC Press; 2013.
75. Tullar IV, Suffet IH. J Air Pollut Control Assoc. 1975; 25:282–286.
76. Nriagu, JO. Vanadium in the environment (Part 1, Chemistry and biochemistry). New York: Wiley; 1998.
77. Mamane, Y., Pirrone, N. Advances in Environmental Science, Technology. Vol. 30. NEW YORK: 1998. p. 37-72.
78. Zenz C, Berg BA. Arch. Environ. Health: An International Journal. 1967; 14:709–712.
79. Rojas E, Valverde M, Herrera L, Altamirano-Lozano M, Ostrosky-Wegman P. Mutat. Res-Envir. Muta. 1996; 359:77–84.
80. Uche F, Obianime A, Gogo-Abite M. J. Appl. Sci. Environ. Manag. 2008:12.
81. Fairhall LT, Dunn RC, Sharpless NE, Pritchard EA. in Public Health Bulletin. 1945:36.
82. Krishnamoorthy K, Premanathan M, Veerapandian M, Kim SJ. Nanotechnology. 2014; 25:315101. [PubMed: 25030310]
83. Xiong J, Cheng G, Li G, Qin F, Chen R. RSC Adv. 2011; 1:1542–1553.
84. Pei L, Yang Y, Pei Y. e-J. Surf. Sci. Nanotech. 2011; 9:297–300.
85. Parnell R. Proc. R. Soc. Med. 1924; 17:19. [PubMed: 19984212]
86. Preussmann R, Ivankovic S. Food Cosmet. Toxicol. 1975; 13:543–544. [PubMed: 1201837]
87. Luckey, TD., Venugopal, B. Physiologic and Chemical Basis for Metal Toxicity. Springer Science & Business Media; 1977.
88. Venugopal, B., Luckey, TD. Metal toxicity in mammals. Volume 2. Chemical toxicity of metals and metalloids. Plenum Press; 1978.
89. Domingo J. J. Toxicol. Environ. Health Part A. 1994; 42:123–141.
90. Chellan P, Sadler PJ. Phil. Trans. R. Soc. A. 2015; 373:20140182. [PubMed: 25666066]
91. Sengupta J, Ghosh S, Datta P, Gomes A, Gomes A. J. Nanosci. Nanotechnol. 2014; 14:990–1006. [PubMed: 24730316]
92. Yokel RA, Lasley SM, Dorman DC. J Toxicol Environ Health B Crit Rev. 2006; 9:63–85. [PubMed: 16393870]
93. Mackler B, Mahler H, Green D. J. Biol. Chem. 1954; 210:149–164. [PubMed: 13201578]
94. Panneerselvam SR, Govindasamy S. Clin. Chim. Acta. 2004; 345:93–98. [PubMed: 15193982]
95. Magos L. Environ. Health Perspect. 1991; 95:157. [PubMed: 1821370]
96. Hayes RB. Cancer Causes & Control. 1997; 8:371–385. [PubMed: 9498900]
97. Mukherjee B, Patra B, Mahapatra S, Banerjee P, Tiwari A, Chatterjee M. Toxicol. Lett. 2004; 150:135–143. [PubMed: 15093669]
98. Gruzewska K, Michno A, Pawelczyk T, Bielarczyk H. J Physiol Pharmacol. 2014; 65:603–611. [PubMed: 25371519]
99. Bertinat R, Nualart F, Li X, Yáñez AJ, Gomis R. J Clin Cell Immunol. 2015; 6:1000285.
100. McInturf S, Bekkedal M, Wilfong E, Arfsten D, Chapman G, Gunasekar P. Toxicol. Appl. Pharmacol. 2011; 254:133–137. [PubMed: 21296100]
101. Sachdeva S, Pant SC, Kushwaha P, Bhargava R, Flora SJ. Food Chem. Toxicol. 2015; 82:64–71. [PubMed: 25983264]

102. Roedel EQ, Cafasso DE, Lee KW, Pierce LM. Toxicol. Appl. Pharmacol. 2012; 259:74–86. [PubMed: 22198552]
103. Nemery B, Abraham JL. Am. J. Respir. Crit. Care Med. 2007; 176:2–3. [PubMed: 17586761]
104. Armstead AL, Arena CB, Li B. Toxicol. Appl. Pharmacol. 2014; 278:1–8. [PubMed: 24746988]
105. Kalinich JF, Emond CA, Dalton TK, Mog SR, Coleman GD, Kordell JE, Miller AC, McClain DE. Environ. Health Perspect. 2005:729–734. [PubMed: 15929896]
106. Santamaria AB, Sulsky SI. J. Toxicol. Environ. Health Part A. 2010; 73:128–155. [PubMed: 20077284]
107. Sano Y, Satoh H, Chiba M, Okamoto M, Serizawa K, Nakashima H, Omae K. J. Occup. Health. 2005; 47:293–298. [PubMed: 16096353]
108. Rodilla V, Miles AT, Jenner W, Hawksworth GM. Chem. Biol. Interact. 1998; 115:71–83. [PubMed: 9817076]
109. Maeda, S., Ohki, A. Wastewater treatment with algae. Springer; 1998. p. 73-92.
110. Wang X, Mansukhani ND, Guiney LM, Ji Z, Chang CH, Wang M, Liao YP, Song TB, Sun B, Li R. Small. 2015; 11:5079–5087. [PubMed: 26237579]
111. Teo WZ, Chng ELK, Sofer Z, Pumera M. Chem. Eur. J. 2014; 20:9627–9632. [PubMed: 24976159]
112. Chng ELK, Sofer Z, Pumera M. Nanoscale. 2014; 6:14412–14418. [PubMed: 25341082]
113. Shah P, Narayanan TN, Li C-Z, Alwarappan S. Nanotechnology. 2015; 26:315102. [PubMed: 26183754]
114. Li Y, Yuan H, von dem Bussche A, Creighton M, Hurt RH, Kane AB, Gao H. Proc. Natl. Acad. Sci. U.S.A. 2013; 110:12295–12300. [PubMed: 23840061]
115. Jachak AC, Creighton M, Qiu Y, Kane AB, Hurt RH. MRS Bull. 2012; 37:1307–1313. [PubMed: 25018584]
116. Smith SC, Rodrigues DF. Carbon. 2015; 91:122–143.
117. Tong T, Shereef A, Wu J, Binh CTT, Kelly JJ, Gaillard J-F. o, Gray KA. Environ. Sci. Technol. 2013; 47:12486–12495. [PubMed: 24083465]
118. Liu S, Hu M, Zeng TH, Wu R, Jiang R, Wei J, Wang L, Kong J, Chen Y. Langmuir. 2012; 28:12364–12372. [PubMed: 22827339]
119. Fan J, Li Y, Nguyen HN, Yao Y, Rodrigues DF. Environ. Sci. Nano. 2015
120. Carpio IEM, Mangadlao JD, Nguyen HN, Advincula RC, Rodrigues DF. Carbon. 2014; 77:289–301.
121. Krishnamoorthy K, Veerapandian M, Yun K, Kim SJ. Colloids Surf B Biointerfaces. 2013; 112:521–524. [PubMed: 24075787]
122. Kou Z, Wang X, Yuan R, Chen H, Zhi Q, Gao L, Wang B, Guo Z, Xue X, Cao W. Nanoscale Res. Lett. 2014; 9:1–9. [PubMed: 24380376]
123. Liu T, Wang C, Gu X, Gong H, Cheng L, Shi X, Feng L, Sun B, Liu Z. Adv. Mater. 2014; 26:3433–3440. [PubMed: 24677423]
124. Qian X, Shen S, Liu T, Cheng L, Liu Z. Nanoscale. 2015; 7:6380–6387. [PubMed: 25786074]
125. Zhang XD, Chen J, Min Y, Park GB, Shen X, Song SS, Sun YM, Wang H, Long W, Xie J. Adv. Funct. Mater. 2014; 24:1718–1729.
126. Song S-S, Xia B-Y, Chen J, Yang J, Shen X, Fan S-J, Guo M-l, Sun Y-M, Zhang X-D. RSC Adv. 2014; 4:42598–42603.
127. Anh Tran T, Krishnamoorthy K, Song YW, Cho SK, Kim SJ. ACS Appl Mater Interfaces. 2014; 6:2980–2986. [PubMed: 24417578]
128. Park M, Lee N, Choi SH, An K, Yu S-H, Kim JH, Kwon S-H, Kim D, Kim H, Baek S-I. Chem. Mater. 2011; 23:3318–3324.
129. Cheng L, Liu J, Gu X, Gong H, Shi X, Liu T, Wang C, Wang X, Liu G, Xing H. Adv. Mater. 2014; 26:1886–1893. [PubMed: 24375758]
130. Li J, Jiang F, Yang B, Song X-R, Liu Y, Yang H-H, Cao D-R, Shi W-R, Chen G-N. Sci. Rep. 2013; 3:1998. [PubMed: 23770650]

131. Elder A, Gelein R, Silva V, Feikert T, Opanashuk L, Carter J, Potter R, Maynard A, Ito Y, Finkelstein J. Environ. Health Perspect. 2006:1172–1178. [PubMed: 16882521]
132. Hussain S, Hess K, Gearhart J, Geiss K, Schlager J. Toxicol. In Vitro. 2005; 19:975–983. [PubMed: 16125895]
133. Chen X, Wu P, Rousseas M, Okawa D, Gartner Z, Zettl A, Bertozzi CR. J. Am. Chem. Soc. 2009; 131:890–891. [PubMed: 19119844]
134. Ciofani G, Danti S, D'Alessandro D, Ricotti L, Moscato S, Bertoni G, Falqui A, Berrettini S, Petrini M, Mattoli V. ACS Nano. 2010; 4:6267–6277. [PubMed: 20925390]
135. Wu H, Yang R, Song B, Han Q, Li J, Zhang Y, Fang Y, Tenne R, Wang C. ACS Nano. 2011; 5:1276–1281. [PubMed: 21230008]
136. Song G, Shen J, Jiang F, Hu R, Li W, An L, Zou R, Chen Z, Qin Z, Hu J. ACS Appl Mater Interfaces. 2014; 6:3915–3922. [PubMed: 24564332]
137. Walker G, Garrett W. Science. 1967; 156:385–387. [PubMed: 17812385]
138. Maisanaba S, Pichardo S, Puerto M, Gutiérrez-Praena D, Cameán AM, Jos A. Environ. Res. 2015; 138:233–254. [PubMed: 25732897]
139. Roggli, VL., Coin, P. Pathology of asbestos-associated diseases. Springer; 2004. p. 1-16.
140. Mandel, G., Mandel, N. Silica silica-induced lung diseases, Boca Raton. New York, London Tokyo: 1996. p. 63-78.
141. Ali F, Reinert L, Lévêque J-M, Duclaux L, Muller F, Saeed S, Shah SS. Ultrason. Sonochem. 2014; 21:1002–1009. [PubMed: 24262759]
142. Pérez-Rodríguez J, Carrera F, Poyato J, Pérez-Maqueda L. Nanotechnology. 2002; 13:382.
143. Sanchez VC, Pietruska JR, Miselis NR, Hurt RH, Kane AB. Wiley Interdiscip Rev Nanomed Nanobiotechnol. 2009; 1:511–529. [PubMed: 20049814]
144. Veblen DR, Wylie AG. Rev Mineral Geochem. 1993; 28:61–137.
145. Heaney PJ, Banfield JF. Rev Mineral Geochem. 1993; 28:185–233.
146. Merget R, Bauer T, Küpper H, Philippou S, Bauer H, Breitstadt R, Bruening T. Arch. Toxicol. 2002; 75:625–634. [PubMed: 11876495]
147. Ross M, Nolan RP, Langer AM, Cooper WC. Rev Mineral Geochem. 1993; 28:361–407.
148. Gibbs A, Pooley F, Griffiths D, Mitha R, Craighead J, Ruttner J. Hum. Pathol. 1992; 23:1344–1354. [PubMed: 1468771]
149. Honma K, Abraham JL, Chiyotani K, De Vuyst P, Dumortier P, Gibbs AR, Green FH, Hosoda Y, Iwai K, Williams WJ. Hum. Pathol. 2004; 35:1515–1523. [PubMed: 15619211]
150. Skulberg KR, Gylseth B, Skaug V, Hanoa R. Scand J Work Environ Health. 1985:65–74. [PubMed: 3890162]
151. Addison J. Regul. Toxicol. Pharm. 1995; 21:397–405.
152. Bandli BR, Gunter ME. Inhal Toxicol. 2006; 18:949–962. [PubMed: 16920668]
153. Fubini B. Environ. Health Perspect. 1997; 105:1013. [PubMed: 9400693]
154. Elmore A. Int. J. Toxicol. 2003; 22:37–102. [PubMed: 12851164]
155. Phillips TD, Afriyie-Gyawu E, Williams J, Huebner H, Ankrah N-A, Ofori-Adjei D, Jolly P, Johnson N, Taylor J, Marroquin-Cardona A. Food Addit. Contam. 2008; 25:134–145.
156. Hooda P, Henry C, Seyoum T, Armstrong L, Fowler M. Environ. Geochem. Health. 2002; 24:305–319.
157. de Sousa Rodrigues LA, Figueiras A, Veiga F, de Freitas RM, Nunes LCC, da Silva Filho EC, da Silva Leite CM. Colloids Surf B Biointerfaces. 2013; 103:642–651. [PubMed: 23253474]
158. Crouch E, Churg A. Am. J. Clin. Pathol. 1983; 80:520–526. [PubMed: 6624719]
159. Donaldson K, Murphy FA, Duffin R, Poland CA. Part Fibre Toxicol. 2010; 7:5. [PubMed: 20307263]
160. Geiser M, Kreyling WG. Part Fibre Toxicol. 2010; 7:1–17. [PubMed: 20180970]
161. Geiser M. Microsc. Res. Tech. 2002; 57:512–522. [PubMed: 12112434]
162. Flannagan RS, Jaumouillé V, Grinstein S. Annu. Rev. Pathol-Mech. 2012; 7:61–98.
163. Hochella, M, Jr. Surface chemistry, structure, and reactivity of hazardous mineral dust. Washington, DC (United States): Mineralogical Society of America; 1993.

164. Keane, MJ., Wallace, WE. Silica and silica-induced lung diseases. Castranov, V.Vallyathan, V., Wallace, WE., editors. Boca Raton: CRC Press; 1995. p. 271-281.
165. Bolsaitis, PP., Wallace, WE. Silica and silica-induced lung diseases. Castranov, V.Vallyathan, V., Wallace, WE., editors. Boca Raton: CRC Press; 1996. p. 79-89.
166. Pavan C, Rabolli V, Tomatis M, Fubini B, Lison D. Part Fibre Toxicol. 2014; 11:1–11. [PubMed: 24382024]
167. Pavan C, Tomatis M, Ghiazza M, Rabolli V, Bolis V, Lison D, Fubini B. Chem. Res. Toxicol. 2013; 26:1188–1198. [PubMed: 23819533]
168. Broaddus VC, Everitt JI, Black B, Kane AB. J Toxicol Environ Health B Crit Rev. 2011; 14:153–178. [PubMed: 21534088]
169. Mossman BT, Lippmann M, Hesterberg TW, Kelsey KT, Barchowsky A, Bonner JC. J Toxicol Environ Health B Crit Rev. 2011; 14:76–121. [PubMed: 21534086]
170. Mossman BT, Shukla A, Heintz NH, Verschraegen CF, Thomas A, Hassan R. Am. J. Pathol. 2013; 182:1065–1077. [PubMed: 23395095]
171. Borm PJ, Schins RP, Albrecht C. Int. J. Cancer. 2004; 110:3–14. [PubMed: 15054863]
172. Borm PJ, Tran L, Donaldson K. Crit. Rev. Toxicol. 2011; 41:756–770. [PubMed: 21923565]
173. Duch MC, Budinger GS, Liang YT, Soberanes S, Urich D, Chiarella SE, Campochiaro LA, Gonzalez A, Chandel NS, Hersam MC. Nano Lett. 2011; 11:5201–5207. [PubMed: 22023654]
174. Yue H, Wei W, Yue Z, Wang B, Luo N, Gao Y, Ma D, Ma G, Su Z. Biomaterials. 2012; 33:4013–4021. [PubMed: 22381473]
175. Oberdörster G, Maynard A, Donaldson K, Castranova V, Fitzpatrick J, Ausman K, Carter J, Karn B, Kreyling W, Lai D, Olin S, Monteiro-Riviere N, Warheit D, Yang H. Part Fibre Toxicol. 2005; 2:1–35. [PubMed: 15813962]
176. Mudunkotuwa IA, Pettibone JM, Grassian VH. Environ. Sci. Technol. 2012; 46:7001–7010. [PubMed: 22280489]
177. Wang Z, von dem Bussche A, Kabadi PK, Kane AB, Hurt RH. ACS Nano. 2013; 7:8715–8727. [PubMed: 24032665]
178. Liu J, Wang Z, Liu FD, Kane AB, Hurt RH. ACS Nano. 2012; 6:9887–9899. [PubMed: 23046098]
179. Liu J, Hurt RH. Environ. Sci. Technol. 2010; 44:2169–2175. [PubMed: 20175529]
180. Sasidharan A, Chandran P, Menon D, Raman S, Nair S, Koyakutty M. Nanoscale. 2011; 3:3657–3669. [PubMed: 21826307]
181. Kim T, Lee K, Gong M-s, Joo S-W. Langmuir. 2005; 21:9524–9528. [PubMed: 16207031]
182. Lynch I, Dawson KA. Nano Today. 2008; 3:40–47.
183. Lowry GV, Gregory KB, Apte SC, Lead JR. Environ. Sci. Technol. 2012; 46:6893–6899. [PubMed: 22582927]
184. Hotze EM, Phenrat T, Lowry GV. J. Environ. Qual. 2010; 39:1909–1924. [PubMed: 21284288]
185. Badawy AME, Luxton TP, Silva RG, Scheckel KG, Suidan MT, Tolaymat TM. Environ. Sci. Technol. 2010; 44:1260–1266. [PubMed: 20099802]
186. Kittler S, Greulich C, Diendorf J, Koller M, Epple M. Chem. Mater. 2010; 22:4548–4554.
187. Su SH, Hsu YT, Chang YH, Chiu MH, Hsu CL, Hsu WT, Chang WH, He H Jr, Li LJ. small. 2014; 10:2589–2594. [PubMed: 24610642]
188. Bissessur R, Kanatzidis MG, Schindler J, Kannewurf C. J. Chem. Soc., Chem. Commun. 1993:1582–1585.
189. Xiu, Z-m, Zhang, Q-b, Puppala, HL., Colvin, VL., Alvarez, PJ. Nano Lett. 2012; 12:4271–4275. [PubMed: 22765771]
190. Karlsson HL, Cronholm P, Gustafsson J, Moller L. Chem. Res. Toxicol. 2008; 21:1726–1732. [PubMed: 18710264]
191. Xia T, Kovochich M, Liong M, Mädler L, Gilbert B, Shi H, Yeh JI, Zink JI, Nel AE. ACS Nano. 2008; 2:2121–2134. [PubMed: 19206459]
192. Zhang H, Ji Z, Xia T, Meng H, Low-Kam C, Liu R, Pokhrel S, Lin S, Wang X, Liao Y-P. ACS Nano. 2012; 6:4349–4368. [PubMed: 22502734]

193. Kirchner C, Liedl T, Kudera S, Pellegrino T, Muñoz Javier A, Gaub HE, Stölzle S, Fertig N, Parak WJ. Nano Lett. 2005; 5:331–338. [PubMed: 15794621]
194. Muñoz A, Costa M. Toxicol. Appl. Pharmacol. 2012; 260:1–16. [PubMed: 22206756]
195. Pietruska JR, Liu X, Smith A, McNeil K, Weston P, Zhitkovich A, Hurt R, Kane AB. Toxicol. Sci. 2011:kfr206.
196. Liu J, Sonshine DA, Shervani S, Hurt RH. ACS Nano. 2010; 4:6903–6913. [PubMed: 20968290]
197. Dehner CA, Barton L, Maurice PA, DuBois JL. Environ. Sci. Technol. 2010; 45:977–983. [PubMed: 21174456]
198. Wang G, Ling Y, Wang H, Yang X, Wang C, Zhang JZ, Li Y. Energy Environ Sci. 2012; 5:6180–6187.
199. Petrochenkov V, Gorichev I, Batrakov V, Izotov A, Kutepov A. Theor. Found. Chem. Eng. 2004; 38:386–393.
200. Baysinger, G. CRC Handbook of Chemistry and Physics. National Institute of Standards and Technology; 2015.
201. Liu B, Zeng HC. J Phys Chem B. 2004; 108:5867–5874.
202. Irmawati R, Shafizah M. Int J Basic Appl Sci. 2009; 9:241–244.
203. Boclair JW, Braterman PS. Chem. Mater. 1999; 11:298–302. [PubMed: 11542280]
204. Chen S, Wang L-W. Chem. Mater. 2012; 24:3659–3666.
205. Gustafsson, JP. Visual MINTEQ version 3.0 http://vminteq.lwr.kth.se/ Stockholm, Sweden. Stockholm, Sweden: 2013.
206. Blinder A, Bolgar A, Trofimova ZA. Powder Metall. Met. Ceram. 1993; 32:234–239.
207. Dellien I. J Chem Thermodyn. 1977; 9:897–900.
208. Kiwia HL, Westrum EF. J Chem Thermodyn. 1975; 7:683–691.
209. Ryzhenko B. Geochem Int. 2010; 48:407–414.
210. Ross S, Sussman A. J Phys Chem. 1955; 59:889–892.
211. Yamamoto M, Dutta S, Aikawa S, Nakaharai S, Wakabayashi K, Fuhrer MS, Ueno K, Tsukagoshi K. Nano Lett. 2015; 15:2067–2073. [PubMed: 25646637]
212. Zhou H, Yu F, Liu Y, Zou X, Cong C, Qiu C, Yu T, Yan Z, Shen X, Sun L, Yakobson B, Tour J. Nano Res. 2013; 6:703–711.
213. Wang, RHZ. presented in part at the SETAC North America 36th Annual Meeting; November 1–5, 2015; Salt Lake City, Utah.
214. Parzinger E, Miller B, Blaschke B, Garrido JA, Ager JW, Holleitner A, Wurstbauer U. ACS Nano. 2015
215. Deng R, Xie X, Vendrell M, Chang Y-T, Liu X. J. Am. Chem. Soc. 2011; 133:20168–20171. [PubMed: 22107163]
216. Herszage J, dos Santos Afonso M, Luther GW. Environ. Sci. Technol. 2003; 37:3332–3338. [PubMed: 12966978]
217. Yamamoto M, Einstein TL, Fuhrer MS, Cullen WG. J Phys Chem C. 2013; 117:25643–25649.
218. Chou SS, De M, Kim J, Byun S, Dykstra C, Yu J, Huang J, Dravid VP. J. Am. Chem. Soc. 2013; 135:4584–4587. [PubMed: 23472859]
219. Raybaud P, Hafner J, Kresse G, Toulhoat H. Phys. Rev. Lett. 1998; 80:1481.
220. Das J, Patra B, Baliarsingh N, Parida K. Appl Clay Sci. 2006; 32:252–260.
221. Mandal S, Mayadevi S. Appl Clay Sci. 2008; 40:54–62.
222. Legrouri A, Lakraimi M, Barroug A, De Roy A, Besse J. Water Res. 2005; 39:3441–3448. [PubMed: 16076477]
223. You Y, Zhao H, Vance GF. Colloids Surf A Physicochem Eng Asp. 2002; 205:161–172.
224. Abate G, Masini JC. Colloids Surf A Physicochem Eng Asp. 2005; 262:33–39.
225. Abollino O, Giacomino A, Malandrino M, Mentasti E. Appl Clay Sci. 2008; 38:227–236.
226. El-Bayaa A, Badawy N, AlKhalik EA. J. Hazard. Mater. 2009; 170:1204–1209. [PubMed: 19524366]

227. Malandrino M, Abollino O, Giacomino A, Aceto M, Mentasti E. J. Colloid Interface Sci. 2006; 299:537–546. [PubMed: 16581085]
228. Yang D, Zheng Z, Liu H, Zhu H, Ke X, Xu Y, Wu D, Sun Y. J Phys Chem C. 2008; 112:16275–16280.
229. Sarina S, Bo A, Liu D, Liu H, Yang D, Zhou C, Maes N, Komarneni S, Zhu H. Chem. Mater. 2014; 26:4788–4795.
230. Li N, Zhang L, Chen Y, Fang M, Zhang J, Wang H. Adv. Funct. Mater. 2012; 22:835–841.
231. Sasaki T, Watanabe M. J. Am. Chem. Soc. 1998; 120:4682–4689.
232. Geng F, Ma R, Ebina Y, Yamauchi Y, Miyamoto N, Sasaki T. J. Am. Chem. Soc. 2014; 136:5491–5500. [PubMed: 24635385]
233. Liu, Z-h, Ooi, K., Kanoh, H., Tang, W-p, Tomida, T. Langmuir. 2000; 16:4154–4164.
234. Han Y-S, Choy J-H. J. Mater. Chem. 2001; 11:1277–1282.
235. Ida S, Ogata C, Eguchi M, Youngblood WJ, Mallouk TE, Matsumoto Y. J. Am. Chem. Soc. 2008; 130:7052–7059. [PubMed: 18461931]
236. Omomo Y, Sasaki T, Wang L, Watanabe M. J. Am. Chem. Soc. 2003; 125:3568–3575. [PubMed: 12643719]
237. Zhu M, Ginder-Vogel M, Sparks DL. Environ. Sci. Technol. 2010; 44:4472–4478. [PubMed: 20469849]
238. Wang Z, Lee S-W, Catalano JG, Lezama-Pacheco JS, Bargar JR, Tebo BM, Giammar DE. Environ. Sci. Technol. 2012; 47:850–858. [PubMed: 23227949]
239. Power LE, Arai Y, Sparks DL. Environ. Sci. Technol. 2005; 39:181–187. [PubMed: 15667093]
240. Crowther DL, Dillard JG, Murray JW. Geochim. Cosmochim. Acta. 1983; 47:1399–1403.
241. Pretorius PJ, Linder PW. Appl. Geochem. 2001; 16:1067–1082.
242. Yuan Y, Li R, Liu Z. Anal. Chem. 2014; 86:3610–3615. [PubMed: 24611524]
243. Darder M, Colilla M, Ruiz-Hitzky E. Chem. Mater. 2003; 15:3774–3780.
244. Yong Y, Zhou L, Gu Z, Yan L, Tian G, Zheng X, Liu X, Zhang X, Shi J, Cong W. Nanoscale. 2014; 6:10394–10403. [PubMed: 25047651]
245. Guan G, Zhang S, Liu S, Cai Y, Low M, Teng CP, Phang IY, Cheng Y, Duei KL, Srinivasan BM. J. Am. Chem. Soc. 2015; 137:6152–6155. [PubMed: 25936424]
246. Heising J, Kanatzidis MG. J. Am. Chem. Soc. 1999; 121:11720–11732.
247. Golub AS, Shumilova IB, Zubavichus YV, Jahncke M, Süss-Fink G, Danot M, Novikov YN. J. Mater. Chem. 1997; 7:163–167.
248. Ollivier P, Mallouk T, Kovtyukhova N, Keller S. Chem. Commun. 1998:1563–1564.
249. Tu Y, Lv M, Xiu P, Huynh T, Zhang M, Castelli M, Liu Z, Huang Q, Fan C, Fang H. Nat. Nano. 2013; 8:594–601.
250. Titov AV, Král P, Pearson R. ACS Nano. 2009; 4:229–234. [PubMed: 20025267]
251. Wang J, Wei Y, Shi X, Gao H. RSC Adv. 2013; 3:15776–15782.
252. Mu Q, Su G, Li L, Gilbertson BO, Yu LH, Zhang Q, Sun Y-P, Yan B. ACS Appl Mater Interfaces. 2012; 4:2259–2266. [PubMed: 22409495]
253. Lammel T, Navas JM. Aquat. Toxicol. 2014; 150:55–65. [PubMed: 24642293]
254. Poland CA, Duffin R, Kinloch I, Maynard A, Wallace WA, Seaton A, Stone V, Brown S, MacNee W, Donaldson K. Nat. Nano. 2008; 3:423–428.
255. Akhavan O, Ghaderi E. ACS Nano. 2010; 4:5731–5736. [PubMed: 20925398]
256. Liao K-H, Lin Y-S, Macosko CW, Haynes CL. ACS Appl Mater Interfaces. 2011; 3:2607–2615. [PubMed: 21650218]
257. Sasidharan A, Panchakarla L, Chandran P, Menon D, Nair S, Rao C, Koyakutty M. Nanoscale. 2011; 3:2461–2464. [PubMed: 21562671]
258. Zhang Y, Ali SF, Dervishi E, Xu Y, Li Z, Casciano D, Biris AS. ACS Nano. 2010; 4:3181–3186. [PubMed: 20481456]
259. Zhou R, Gao H. Wiley Interdiscip Rev Nanomed Nanobiotechnol. 2014; 6:452–474. [PubMed: 24957946]

260. Li Y, Liu Y, Fu Y, Wei T, Le Guyader L, Gao G, Liu R-S, Chang Y-Z, Chen C. Biomaterials. 2012; 33:402–411. [PubMed: 22019121]
261. Chang Y, Yang S-T, Liu J-H, Dong E, Wang Y, Cao A, Liu Y, Wang H. Toxicol. Lett. 2011; 200:201–210. [PubMed: 21130147]
262. Liu J, Yang Z, Li H, Gu Z, Garate JA, Zhou R. J. Chem. Phys. 2014; 141 22D520.
263. Luan B, Huynh T, Zhao L, Zhou R. ACS Nano. 2014; 9:663–669. [PubMed: 25494677]
264. Akhavan O, Ghaderi E, Akhavan A. Biomaterials. 2012; 33:8017–8025. [PubMed: 22863381]
265. Hashemi E, Akhavan O, Shamsara M, Valimehr S, Rahighi R. RSC Adv. 2014; 4:60720–60728.
266. Yuan J, Gao H, Sui J, Duan H, Chen WN, Ching CB. Toxicol. Sci. 2012; 126:149–161. [PubMed: 22157353]
267. Carpio IEM, Santos CM, Wei X, Rodrigues DF. Nanoscale. 2012; 4:4746–4756. [PubMed: 22751735]
268. Chen J, Peng H, Wang X, Shao F, Yuan Z, Han H. Nanoscale. 2014; 6:1879–1889. [PubMed: 24362636]
269. Hui L, Piao J-G, Auletta J, Hu K, Zhu Y, Meyer T, Liu H, Yang L. ACS Appl Mater Interfaces. 2014; 6:13183–13190. [PubMed: 25026597]
270. Liu S, Zeng TH, Hofmann M, Burcombe E, Wei J, Jiang R, Kong J, Chen Y. ACS Nano. 2011; 5:6971–6980. [PubMed: 21851105]
271. Perreault F, de Faria AF, Nejati S, Elimelech M. ACS nano. 2015; 9:7226–7236. [PubMed: 26091689]
272. Sametband M, Kalt I, Gedanken A, Sarid R. ACS Appl Mater Interfaces. 2014; 6:1228–1235. [PubMed: 24364493]
273. Ye S, Shao K, Li Z, Guo N, Zuo Y, Li Q, Lu Z, Chen L, He Q, Han H. ACS Appl Mater Interfaces. 2015; 7:21571–21579. [PubMed: 26370151]
274. Sawangphruk M, Srimuk P, Chiochan P, Sangsri T, Siwayaprahm P. Carbon. 2012; 50:5156–5161.
275. Wang X, Liu X, Chen J, Han H, Yuan Z. Carbon. 2014; 68:798–806.
276. Hu X, Lu K, Mu L, Kang J, Zhou Q. Carbon. 2014; 80:665–676.
277. Nogueira P, Nakabayashi D, Zucolotto V. Aquat. Toxicol. 2015; 166:29–35. [PubMed: 26204245]
278. Pretti C, Oliva M, Di Pietro R, Monni G, Cevasco G, Chiellini F, Pomelli C, Chiappe C. Ecotoxicol. Environ. Saf. 2014; 101:138–145. [PubMed: 24507139]
279. Wahid MH, Eroglu E, Chen X, Smith SM, Raston CL. RSC Adv. 2013; 3:8180–8183.
280. Hu C, Wang Q, Zhao H, Wang L, Guo S, Li X. Chemosphere. 2015; 128:184–190. [PubMed: 25703902]
281. Wang Z, Tonderys D, Leggett SE, Williams EK, Kiani MT, Steinberg RS, Qiu Y, Wong IY, Hurt RH. Carbon. 2016; 97:14–24. [PubMed: 25848137]
282. Boal, D., Boal, DH. Mechanics of the Cell. Cambridge University Press; 2012.
283. Guo R, Mao J, Yan L-T. Biomaterials. 2013; 34:4296–4301. [PubMed: 23489926]
284. Mao J, Guo R, Yan L-T. Biomaterials. 2014; 35:6069–6077. [PubMed: 24780168]
285. Yi X, Gao H. Nanoscale. 2015; 7:5457–5467. [PubMed: 25732111]
286. Kudin KN, Scuseria GE, Yakobson BI. Phys. Rev. B. 2001; 64:235406.
287. Wei Y, Wang B, Wu J, Yang R, Dunn ML. Nano Lett. 2012; 13:26–30. [PubMed: 23214980]
288. Lee C, Wei X, Kysar JW, Hone J. Science. 2008; 321:385–388. [PubMed: 18635798]
289. Wei X, Fragneaud B, Marianetti CA, Kysar JW. Phys. Rev. B. 2009; 80:205407.
290. Wu J, Wang B, Wei Y, Yang R, Dresselhaus M. Mater.Res. Lett. 2013; 1:200–206.
291. Peng Q, Ji W, De S. Comp. Mater. Sci. 2012; 56:11–17.
292. Song L, Ci L, Lu H, Sorokin PB, Jin C, Ni J, Kvashnin AG, Kvashnin DG, Lou J, Yakobson BI. Nano Lett. 2010; 10:3209–3215. [PubMed: 20698639]
293. Kim KK, Hsu A, Jia X, Kim SM, Shi Y, Hofmann M, Nezich D, Rodriguez-Nieva JF, Dresselhaus M, Palacios T. Nano Lett. 2011; 12:161–166. [PubMed: 22111957]
294. Jiang J-W, Qi Z, Park HS, Rabczuk T. Nanotechnology. 2013; 24:435705. [PubMed: 24084656]
295. Bertolazzi S, Brivio J, Kis A. ACS Nano. 2011; 5:9703–9709. [PubMed: 22087740]

296. Cooper RC, Lee C, Marianetti CA, Wei X, Hone J, Kysar JW. Phys. Rev. B. 2013; 87:035423.
297. Radisavljevic B, Radenovic A, Brivio J, Giacometti V, Kis A. Nat. Nano. 2011; 6:147–150.
298. Cranford SW, Buehler MJ. Carbon. 2011; 49:4111–4121.
299. Kang J, Li J, Wu F, Li S-S, Xia J-B. J Phys Chem C. 2011; 115:20466–20470.
300. Peng Q, Ji W, De S. Phys. Chem. Chem. Phys. 2012; 14:13385–13391. [PubMed: 22941420]
301. Cao C, Daly M, Singh CV, Sun Y, Filleter T. Carbon. 2015; 81:497–504.
302. Suk JW, Piner RD, An J, Ruoff RS. ACS Nano. 2010; 4:6557–6564. [PubMed: 20942443]
303. Marsh D. Chem. Phys. Lipids. 2006; 144:146–159. [PubMed: 17045578]
304. Rawicz W, Olbrich K, McIntosh T, Needham D, Evans E. Biophys. J. 2000; 79:328–339. [PubMed: 10866959]
305. Evans E, Heinrich V, Ludwig F, Rawicz W. Biophys. J. 2003; 85:2342–2350. [PubMed: 14507698]
306. Hategan A, Law R, Kahn S, Discher DE. Biophys. J. 2003; 85:2746–2759. [PubMed: 14507737]
307. Gracià RS, Bezlyepkina N, Knorr RL, Lipowsky R, Dimova R. Soft Matter. 2010; 6:1472–1482.
308. Dao M, Li J, Suresh S. Mater. Sci. Eng. C. 2006; 26:1232–1244.
309. Kempaiah R, Chung A, Maheshwari V. ACS Nano. 2011; 5:6025–6031. [PubMed: 21675743]
310. Kempaiah R, Salgado S, Chung WL, Maheshwari V. Chem. Commun. 2011; 47:11480–11482.
311. Wang B, Liu P, Jiang W, Pan H, Xu X, Tang R. Angew. Chem. Int. Ed. 2008; 47:3560–3564.
312. Yang SH, Lee T, Seo E, Ko EH, Choi IS, Kim BS. Macromol. Biosci. 2012; 12:61–66. [PubMed: 22028147]
313. Seifert U. Adv. Phys. 1997; 46:13–137.
314. Helfrich W. Z. Naturforsch. C. 1973; 28:693–703. [PubMed: 4273690]
315. Zhong-Can O-Y, Helfrich W. Phys. Rev. A. 1989; 39:5280.
316. Yi X, Shi X, Gao H. Phys. Rev. Lett. 2011; 107:098101. [PubMed: 21929271]
317. Yamaki N. J. Appl. Mech. 1958; 25:267–273.
318. Nel AE, Mädler L, Velegol D, Xia T, Hoek EM, Somasundaran P, Klaessig F, Castranova V, Thompson M. Nat. Mater. 2009; 8:543–557. [PubMed: 19525947]
319. Voiry D, Salehi M, Silva R, Fujita T, Chen M, Asefa T, Shenoy VB, Eda G, Chhowalla M. Nano Lett. 2013; 13:6222–6227. [PubMed: 24251828]
320. Lin H, Li L, Zhao M, Huang X, Chen X, Li G, Yu R. J. Am. Chem. Soc. 2012; 134:8328–8331. [PubMed: 22559221]
321. Xiao W, Wang D, Lou XW. J Phys Chem C. 2009; 114:1694–1700.
322. Burello E, Worth AP. Nanotoxicology. 2011; 5:228–235. [PubMed: 21609138]
323. Plumlee GS, Morman SA, Ziegler TL. Rev Mineral Geochem. 2006; 64:5–57.
324. Liu X, Sen S, Liu J, Kulaots I, Geohegan D, Kane A, Puretzky AA, Rouleau CM, More KL, Palmore GTR, Hurt RH. Small. 2011; 7:2775–2785. [PubMed: 21818846]
325. Manna SK, Sarkar S, Barr J, Wise K, Barrera EV, Jejelowo O, Rice-Ficht AC, Ramesh GT. Nano Lett. 2005; 5:1676–1684. [PubMed: 16159204]
326. Song SH, Kim BH, Choe D-H, Kim J, Kim DC, Lee DJ, Kim JM, Chang KJ, Jeon S. Adv. Mater. 2015; 27:3152–3158. [PubMed: 25867545]
327. Hui YY, Liu X, Jie W, Chan NY, Hao J, Hsu Y-T, Li L-J, Guo W, Lau SP. ACS Nano. 2013; 7:7126–7131. [PubMed: 23844893]
328. Kim SS, Khai TV, Kulish V, Kim Y-H, Na HG, Katoch A, Osada M, Wu P, Kim HW. Chem. Mater. 2015; 27:4222–4228.
329. Gong Y, Liu Z, Lupini AR, Shi G, Lin J, Najmaei S, Lin Z, Elías AL, Berkdemir A, You G. Nano Lett. 2013; 14:442–449. [PubMed: 24368045]
330. Mouri S, Miyauchi Y, Matsuda K. Nano Lett. 2013; 13:5944–5948. [PubMed: 24215567]
331. Partoens B, Peeters FM. Phys. Rev. B. 2006; 74:075404.
332. Odom TW, Huang J-L, Kim P, Lieber CM. Nature. 1998; 391:62–64.
333. Gong C, Zhang H, Wang W, Colombo L, Wallace RM, Cho K. Appl. Phys. Lett. 2013; 103:053513.

334. Shirodkar SN, Waghmare UV, Fisher TS, Grau-Crespo R. Phys. Chem. Chem. Phys. 2015; 17:13547–13552. [PubMed: 25940395]
335. Sakai N, Ebina Y, Takada K, Sasaki T. J Phys Chem B. 2005; 109:9651–9655. [PubMed: 16852162]
336. Sakai N, Ebina Y, Takada K, Sasaki T. J. Am. Chem. Soc. 2004; 126:5851–5858. [PubMed: 15125677]
337. Greiner MT, Helander MG, Tang W-M, Wang Z-B, Qiu J, Lu Z-H. Nat. Mater. 2012; 11:76–81. [PubMed: 22057388]
338. Wood PM. Biochem. J. 1988; 253:287. [PubMed: 2844170]
339. Lanphere JD, Luth CJ, Guiney LM, Mansukhani ND, Hersam MC, Walker SL. Environ. Eng. Sci. 2015; 32:163–173. [PubMed: 25741176]
340. Colvin VL. Nat. Biotechnol. 2003; 21:1166–1170. [PubMed: 14520401]
341. Klaine SJ, Alvarez PJ, Batley GE, Fernandes TF, Handy RD, Lyon DY, Mahendra S, McLaughlin MJ, Lead JR. Environ. Toxicol. Chem. 2008; 27:1825–1851. [PubMed: 19086204]
342. Bertino DJ, Zepp RG. Environ. Sci. Technol. 1991; 25:1267–1273.
343. Catts JG, Langmuir D. Appl. Geochem. 1986; 1:255–264.
344. Cofer CG, Economy J. Carbon. 1995; 33:389–395.
345. Dong L, Zhu Z, Ma H, Qiu Y, Zhao J. J. Environ. Sci. 2010; 22:225–229.
346. Kim E-J, Lee C-S, Chang Y-Y, Chang Y-S. ACS Appl Mater Interfaces. 2013; 5:9628–9634. [PubMed: 24028422]
347. Remucal CK, Ginder-Vogel M. Environ. Sci. Process Impacts. 2014; 16:1247–1266. [PubMed: 24791271]
348. Sunda WG, Huntsman SA, Harvey GR. Nature. 1983; 301:234–236.
349. Bosecker K. FEMS Microbiol. Rev. 1997; 20:591–604.
350. Bryner L, Anderson R. Ind. Eng. Chem. 1957; 49:1721–1724.
351. Schippers A, Sand W. Appl. Environ. Microbiol. 1999; 65:319–321. [PubMed: 9872800]
352. Tributsch H, Bennett JC. J. Chem. Technol. Biotechnol. 1981; 31:627–635.
353. Liu J, Li X-B, Wang D, Lau W-M, Peng P, Liu L-M. J. Chem. Phys. 2014; 140:054707. [PubMed: 24511968]
354. Joy PA, Vasudevan S. J. Am. Chem. Soc. 1992; 114:7792–7801.
355. Evans JSO, O'Hare D. Adv. Mater. 1994; 6:646–648.
356. Westreich P, Yang D, Frindt RF. Mater. Res. Bull. 2006; 41:502–514.
357. Brec, R. Intercalation in Layered Materials. Springer; 1986. p. 93-124.
358. Ruiz-León D, Manríquez V, Kasaneva J, Avila RE. Mater. Res. Bull. 2002; 37:981–989.
359. Venkataraman NV, Mohanambe L, Vasudevan S. J. Mater. Chem. 2003; 13:170–171.
360. Musumeci AW, Schiller TL, Xu ZP, Minchin RF, Martin DJ, Smith SV. J Phys Chem C. 2010; 114:734–740.
361. Stumm W, Wollast R. Rev. Geophys. 1990; 28:53–69.
362. Goodman BA, Cheshire MV. Nature. 1982; 299:618–620.
363. Golden D, Dixon J, Chen C. Clays Clay Miner. 1986; 34:511–520.
364. Golden D, Chen C, Dixon J. Science. 1986; 231:717–719. [PubMed: 17800797]
365. Wang Y, Feng X, Villalobos M, Tan W, Liu F. Chem. Geol. 2012; 292–293:25–34.
366. Landing WM, Bruland KW. Earth Planet. Sci. Lett. 1980; 49:45–56.
367. Godtfredsen KL, Stone AT. Environ. Sci. Technol. 1994; 28:1450–1458. [PubMed: 22165928]
368. Klausen J, Haderlein SB, Schwarzenbach RP. Environ. Sci. Technol. 1997; 31:2642–2649.
369. Liu CS, Zhang LJ, Feng CH, Wu CA, Li FB, Li XZ. Environ. Chem. 2009; 6:83–92.
370. Marafatto FF, Strader ML, Gonzalez-Holguera J, Schwartzberg A, Gilbert B, Peña J. Proc. Natl. Acad. Sci. U.S.A. 2015; 112:4600–4605. [PubMed: 25825757]
371. Liu Z, Gong Y, Zhou W, Ma L, Yu J, Idrobo JC, Jung J, MacDonald AH, Vajtai R, Lou J. Nat. Commun. 2013:4.

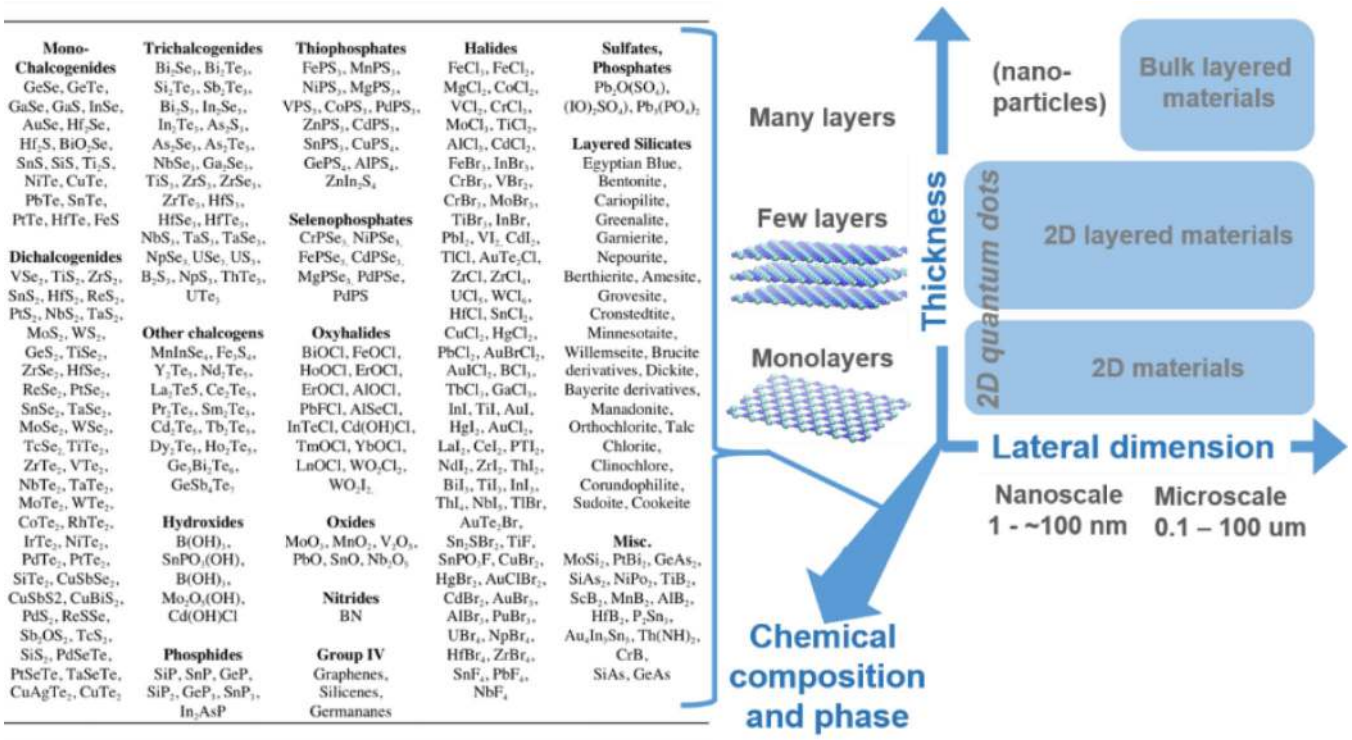


**Figure 1.**

Diversity in chemistry and morphology of 2D and layered materials. Right: Classification of 2D materials used in this review. Morphology (thickness and lateral dimension) together with chemical composition and phase are co-determinants of biological and environmental behavior. Left: Examples of 2D and layered material compositions, illustrating the high degree of chemical diversity.

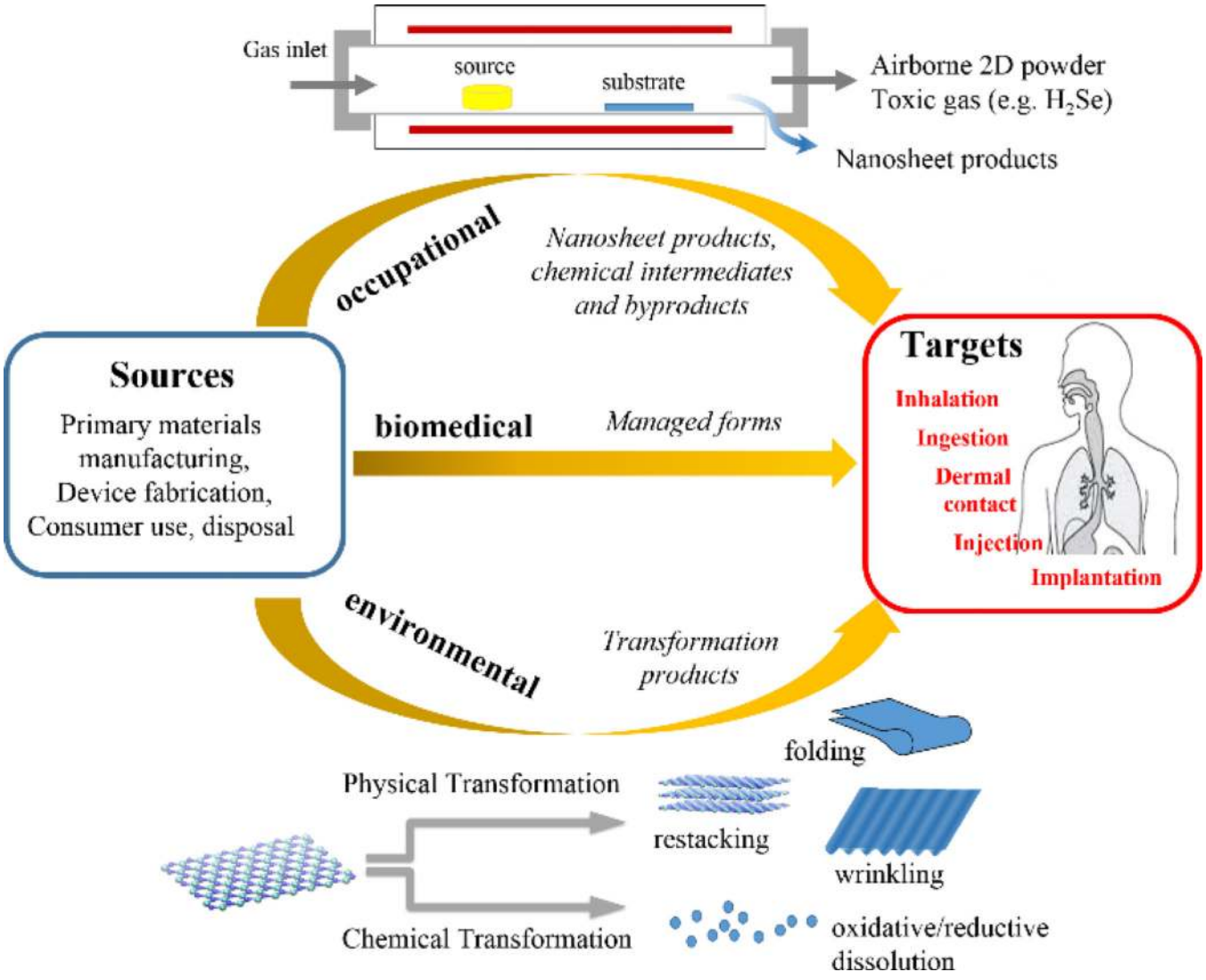


**Figure 2.**

Exposure types and pathways for emerging 2D nanomaterials. Most behaviors and issues are similar to those for particulate nanomaterials,[21] but there are also distinctive 2D behaviors as shown here, such as physical transformations by folding, wrinkling, and restacking, and the importance of hazardous chemical byproducts and reductive dissolution processes associated with the particular chemical compositions of some important inorganic nanosheet materials.

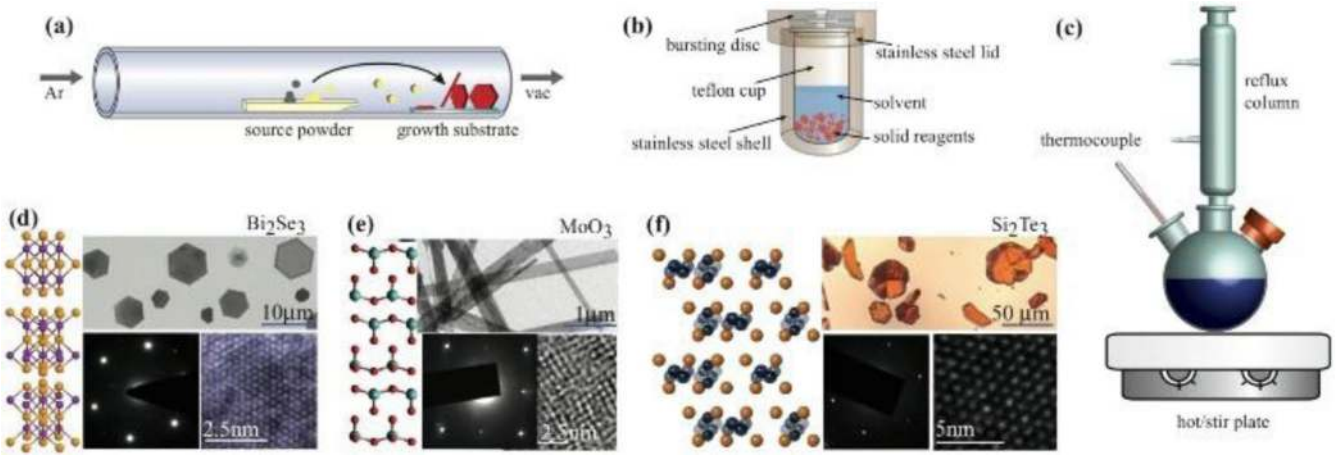


**Figure 3.**

Common synthetic routes to 2D materials. (a) Vapor-phase synthesis, (b) solvothermal/hydrothermal solution synthesis, (c) colloidal solution-based growth. (d) Example $Bi_2Se_3$ plates (1–5nm thick) synthesized through solvothermal growth.[30] Adapted with permission from ref. 30. Copyright 2013 American Chemical Society. (e) $MoO_3$ nanoribbons synthesized through hydrothermal growth.[32] Adapted with permission from ref. 32. Copyright 2015 American Chemical Society. (f) vapor-phase synthesized silicon telluride, $Si_2Te_3$.[33] Adapted with permission from ref. 33. Copyright 2015 American Chemical Society.

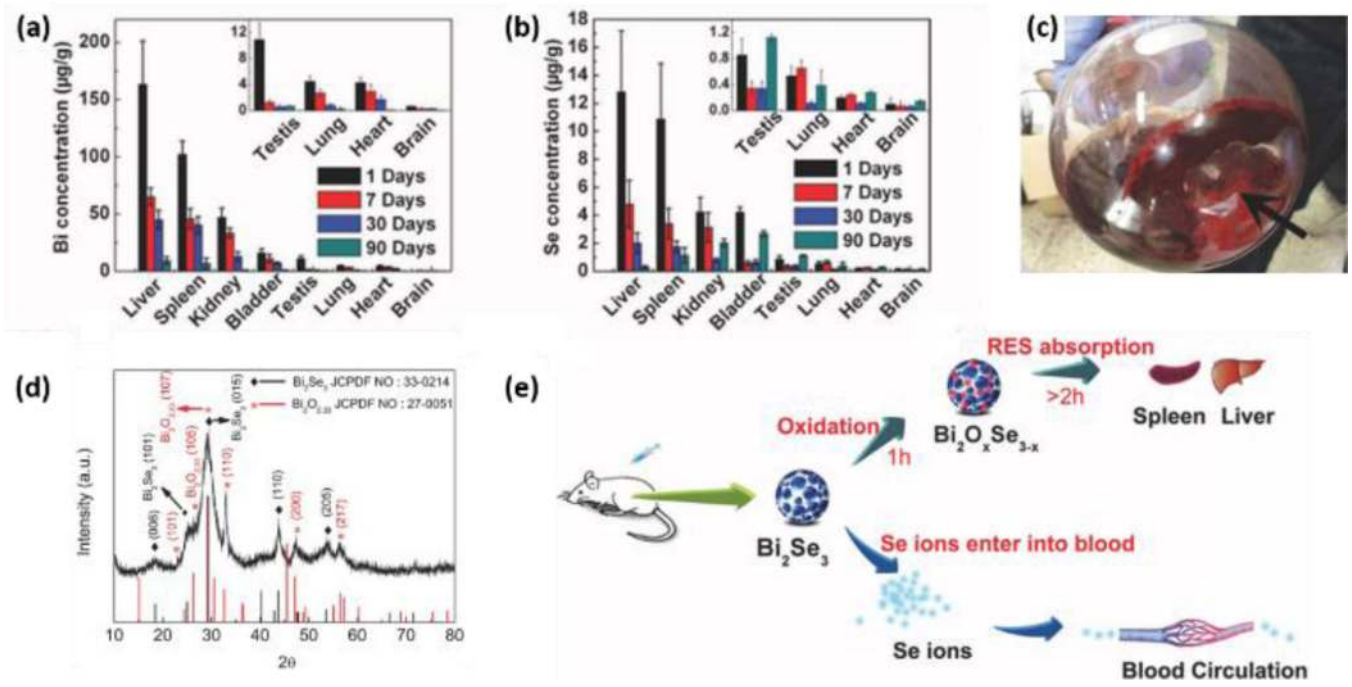


**Figure 4.**

*In vivo* clearance of elemental Bi and Se and oxidation/dissolution of $Bi_2Se_3$ nanosheets. Time-depnedent decrease of Bi concentratoin (a) and Se concentration (b) caused by clearance effects. Digital image (c) and XRD spectrum of the oxidized $Bi_2Se_3$ nanosheets after exposure to air for 30 days (d). (e) Illustration showing dissolution and oxidation of the $Bi_2Se_3$ nanosheets after intraperitoneal injection. Reprinted with permission from ref. 125. Copyright 2013, John Wiley & Sons, Inc.

**Pathologic Reactions Following Inhalation of Silicate Mineral Dusts**

Widespread severe reactions (+++); focal reactions (++); limited reactions (+); no reactions reported (-)

| | Lung Reactions | | | Pleural Reactions | |
|---|---|---|---|---|---|
| **Material (Dust)** | **Fibrosis** | **Granul-omas** | **Lung Cancer** | **Fibrosis** | **Malignant Mesothelioma** |
| **Silicate Particles** Crystalline Silica | ++ | – | Established epidemiol. evidence | + | – |
| Amorphous Silica | – | – | – | – | – |
| **Fibrous Silicates** Asbestos | +++ | – | Established epidemiol. evidence | +++ | Established epidemiological evidence |
| Wollastonite | – | – | – | – | – |
| **Sheet or Plate-like Silicates** Talc; $(Mg_3)(Si_2O_5)_2(OH_2)$ | + | + | – | – | – |
| Mica (Biotite) $[(MgFe)_3(Si_3Al)O_{10}(OH)_2]K$ | + | + | – | + | – |
| Kaolinite; $[Al_4Si_4O_{10}](OH)_8$ | + | + | – | + | – |
| Montmorillonite $[(MgFe)_3(Si_3Al)O_{10}(OH)_2]K$ | + | – | – | – | – |
| Sepiolite; $Mg_4Si_6O_{15}(OH)_26H_2O$ | – | – | – | – | – |
| Attapulgite $(Mg, Al)_2, i_4O_{10}(OH).4(H_2O)$ | – | – | – | – | – |
| Vermiculite $[Mg_5.Si_6Al_2/O_{20}(OH)_4][M^{n+}{}_{1/n}](Mg_5)$ | – | – | – | – | – |

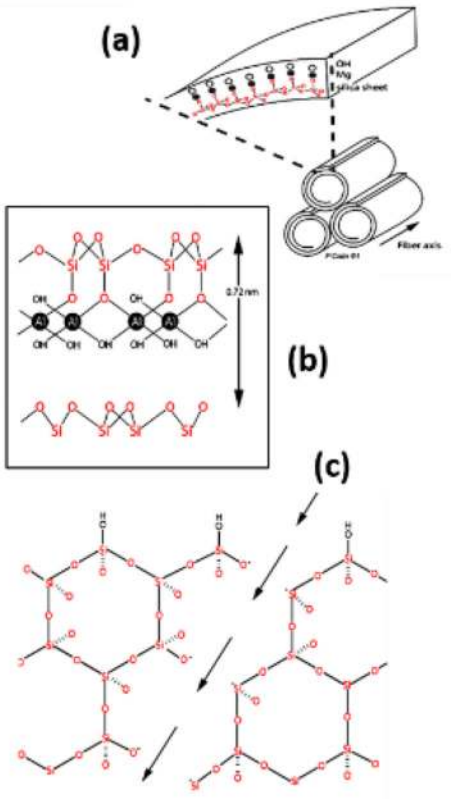


**Figure 5.**

Structure and human health effects of sheet-like silicate minerals. Table 2 summarizes the known pathological responses to inhalation as a function of material type. (a) Crystal structure of chrysotile asbestos.[139] Reprinted with permission from ref. 139. Copyright 2004, Springer. (b) Crystal structure of kaolinite, which is a 2D silicate clay mineral. (c) Lattice of crystalline silica or α-quartz. Fracturing the crystal along the arrows generates highly reactive Si• or SiO• dangling bonds on the new surface.[140] Reprinted with permission from ref. 140. Copyright 1996, Taylor & Francis.

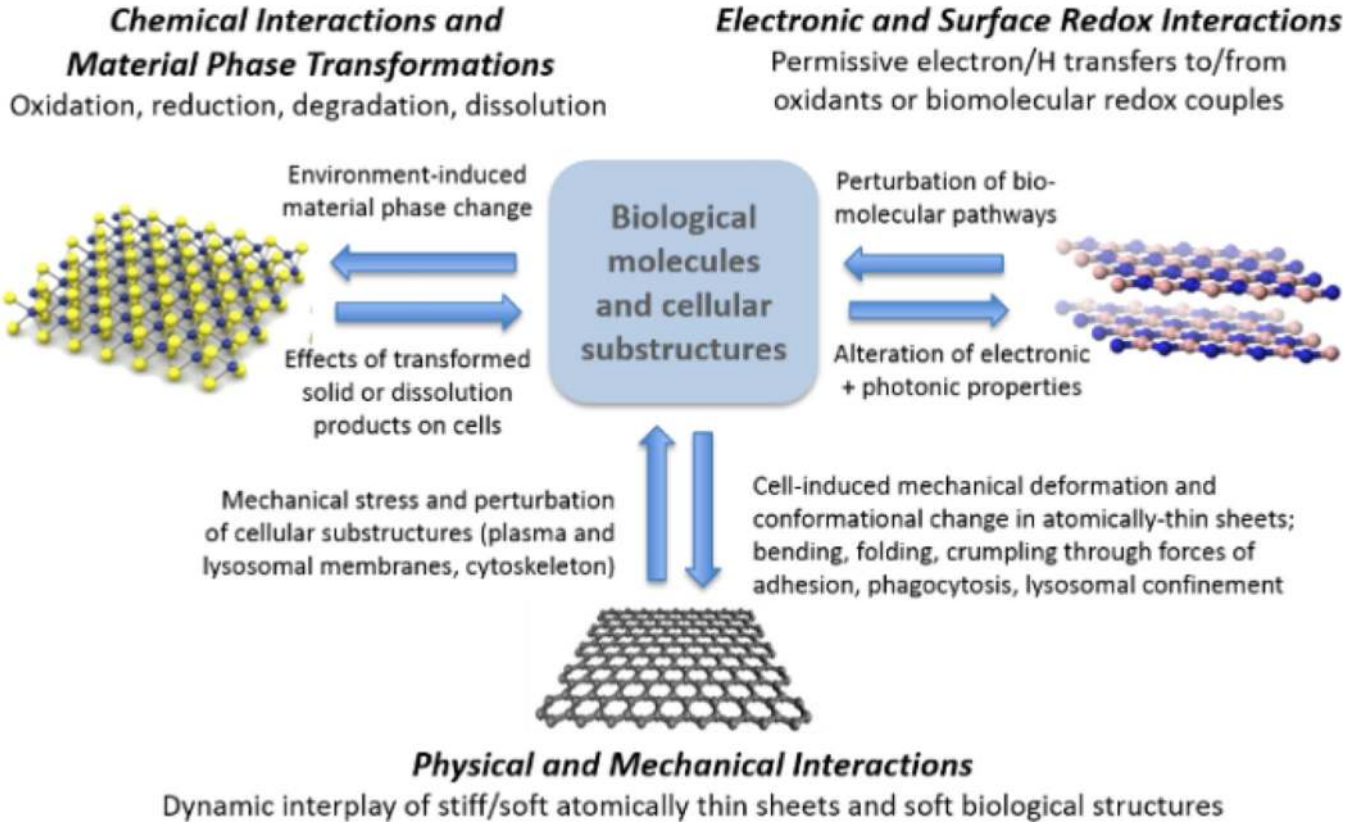


**Figure 6.**

Fundamental modes of interaction between 2D materials and biological systems. The arrows show the *bidirectionality* of the interactions, in which the biological environment induces chemical or physical material transformations, while the materials and/or their transformation products induce biological responses.

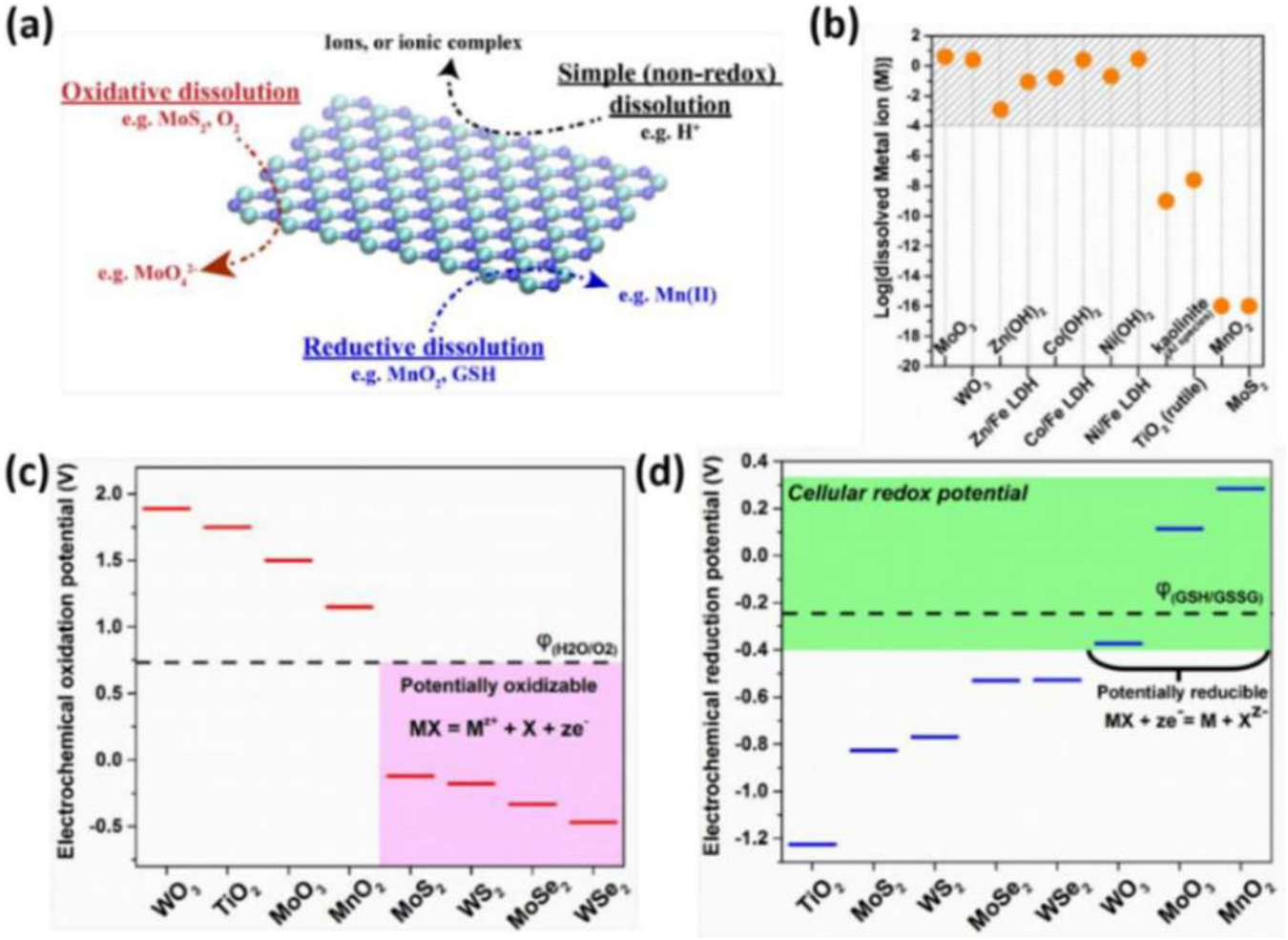


**Figure 7.**

Dissolution behaviors of 2D nanomaterials. (a) Three dissolution mechanisms in biological and environmental media. (b) Equilibrium solubilities of metal sulfides, oxides, hydroxides and LDHs at pH 7 based on solubility constants for metal hydroxides and LAHs,[203] or Visual MINTEQ 3.1 for metal oxides and sulfides at pH 7 with 1 mM $NaNO_3$ as electrolyte.[205] (c) Criterion for oxidative dissolution: comparison of 2D material oxidation potentials with the water/$O_2$ redox couple (pH 7), suggesting that $MoS_2$, $MoSe_2$, $WS_2$ and $WSe_2$ are likely to be oxidatively unstable. (d) Criterion for reductive dissolution: comparison of 2D material reduction potential with the cellular redox potential (exemplified by GSH/GSSG couple) at pH 7, suggesting $WO_3$, $MoO_3$ and $MnO_2$ are unstable to biological reduction and dissolution.

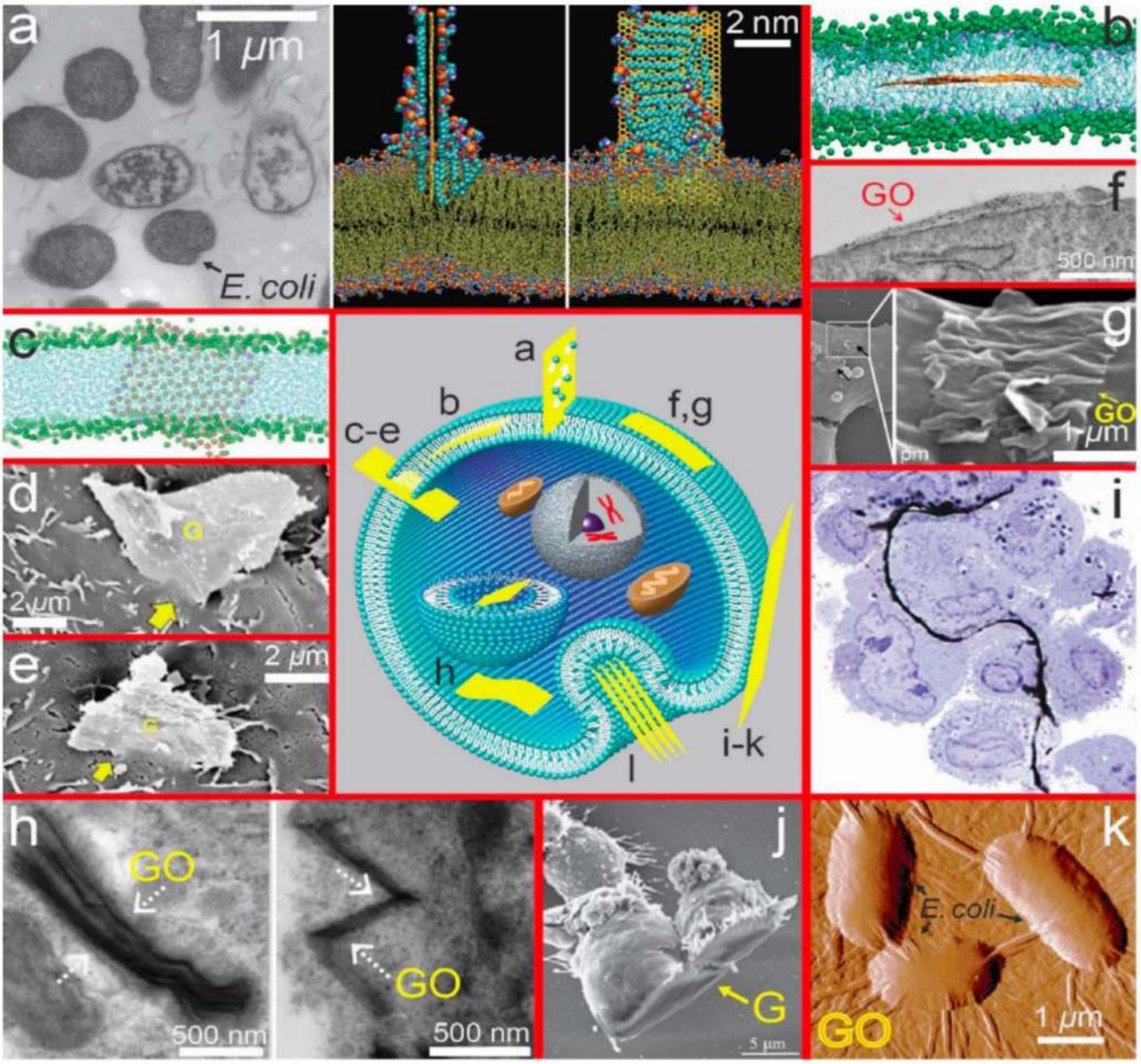


**Figure 8.**

Physical and mechanical modes of 2D material bio-interactions, illustrated using data on graphene (G) and graphene oxide (GO). (a) Experimental observation and molecular dynamics simulations on the destructive extractions of lipid molecules from *E. coli* lipid membranes after incubations with graphene nanosheets. Reprinted by permission from Macmillan Publishers Ltd: Nat. Nanotechnol.,[249] copyright 2013. (b) A pristine graphene nanoflake (6×6 nm) aligns parallel at the interface between two lipid monolayers.[250] Reprinted with permission from ref. 250. Copyright 2009 American Chemical Society. (c) A graphene nanoflake (5.5×6 nm) with 10% of edge carbon atoms oxidized adopts a near-perpendicular transmembrane configuration.[251] The lipid molecules are shown in cyan with green head groups. Reproduced from Ref. 251 with permission from The Royal Society of

Chemistry. Corner penetration (d) and edge penetration (e) of a graphene microsheet into a primary human keratinocyte.[114] Copyright (2013) National Academy of Sciences, USA. (f) Protein-coated GO sheets adhere parallel onto the surface of mouse C2C12 mesenchymal cells followed by subsequent cellular internalization.[252] Reprinted with permission from ref. 252. Copyright 2012 American Chemical Society. (g) Large GO sheets (yellow arrow) attach to the plasma membrane of fish liver cells (PLHC-1). Wrinkles are formed due to the large lateral size of the adhering GO sheets.[253] Reprinted with permission from ref. 253. Copyright 2012 Elsevier Ltd. (h) After initial internalization by peritoneal macrophages, GO sheets of lateral size 2 μm undergo significant deformation and exhibit wrinkling.[174] Reprinted with permission from ref. 174. Copyright 2012 Elsevier Ltd. (i) Few-layer graphene sheets wrap around human THP-1 macrophages.[19] (j) Human THP-1 macrophages adhere to and then spread along the surface of 25 μm few-layer graphene sheets.[19] (i) and (j) reprinted with permission from ref. 19. Copyright 2012 American Chemical Society. (k) AFM images of *E. coli* cells covered by large GO sheets of average lateral size 13 $\mu m^2$.[118] Reprinted with permission from ref. 118. Copyright 2012 American Chemical Society. The central panel is a schematic representation of the above interaction modes (a-k) as well as endocytosis (l) by which (multilayer) 2D materials could possibly enter the cell.

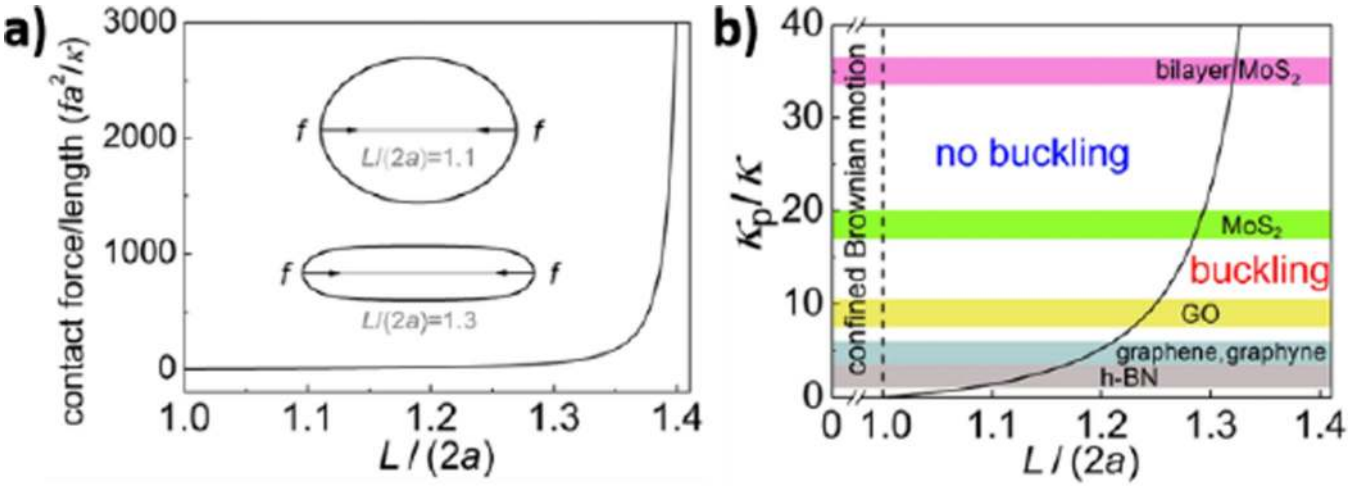


**Figure 9.**

Mechanical interaction between an internalized circular sheet of diameter $L$ and a surrounding vesicle of effective radius $a$ at zero osmotic pressure. (a) Compressive contact force $f$ between the vesicle membrane and encapsulated sheet (assumed to be rigid in the contact force calculation). (b) Buckling phase diagram with respect to the length ratio $L/(2a)$ and bending stiffness ratio $\kappa_p/\kappa$. Insets in (a) correspond to the vesicle configurations at $L/(2a)$=1.1 and 1.3. Colored strips in (b) mark the regimes in which the corresponding 2D materials would buckle beyond a critical length. Except the bilayer $MoS_2$ in the magenta regime, the other 2D materials marked in (b) are of monolayer structures. In the case of lateral size $L<2a$, the encapsulated 2D material would undergo random Brownian motion in the vesicular confinement.

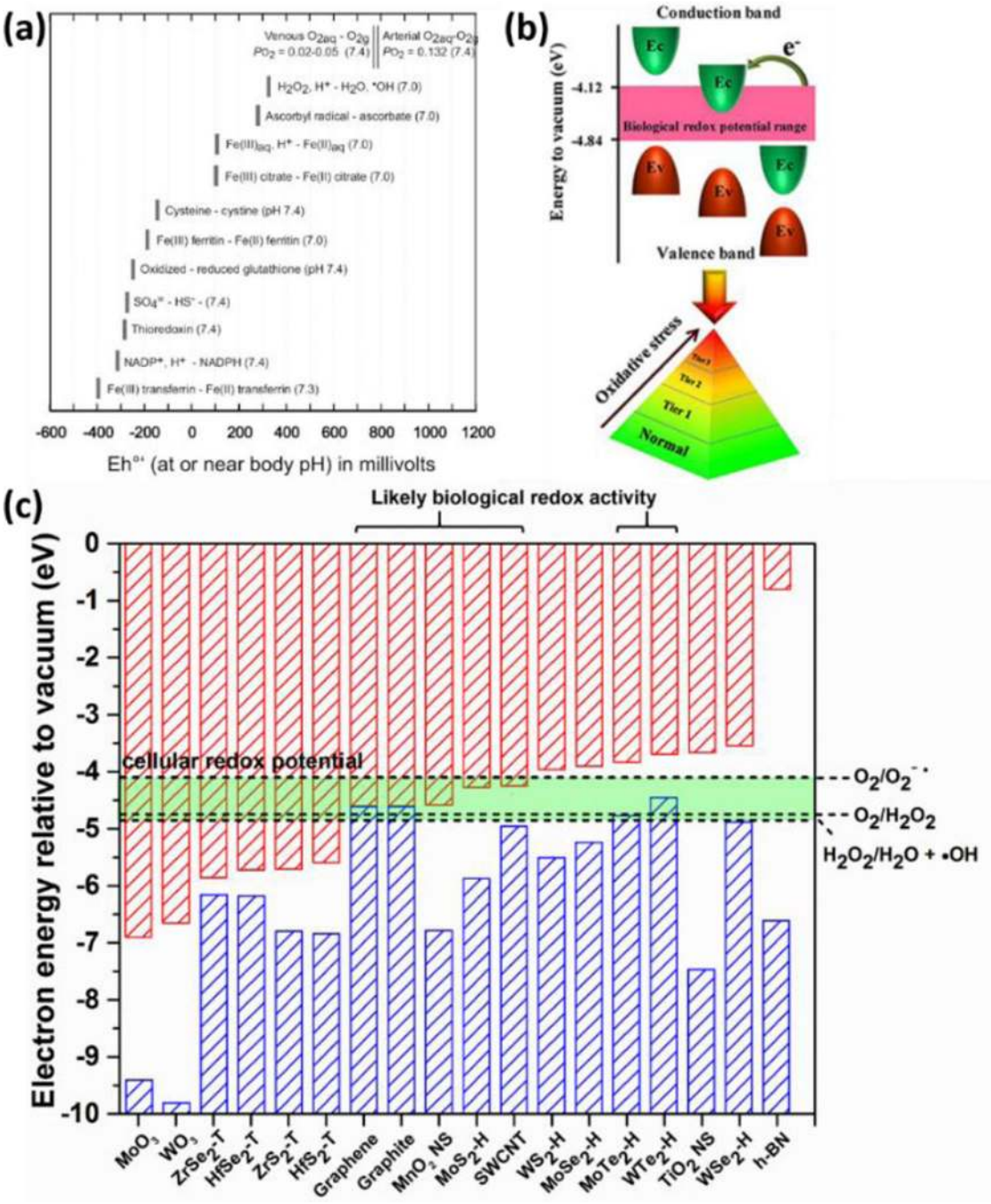


**Figure 10.**

Band structures of 2D and bulk layered materials, and band alignment with the cellular redox potential and the ROS-involved redox couples. (a) Cellular redox potential range defined by biomolecular redox couples. Reprinted with permission from ref. 323. Copyright 2006 Mineralogical Society of America. (b) The illustration of platform for modeling of structure–activity relationships based on band structures. Reprinted with permission from ref. 192 Copyright 2012 American Chemical Society. (c) The comparison a physicochemical *in silico* screening tool for identifying specific 2D materials with high potential for

biological redox activity. Construction of the framework is based on published data in graphite,[331] single wall carbon nanotubes,[332] TMD,[333] h-BN,[334] $MnO_2$ nanosheets,[335] lepidocrocite-type $TiO_2$ nanosheets,[336] $MoO_3$ and $WO_3$,[337] and ROS-involved redox couples.[338]

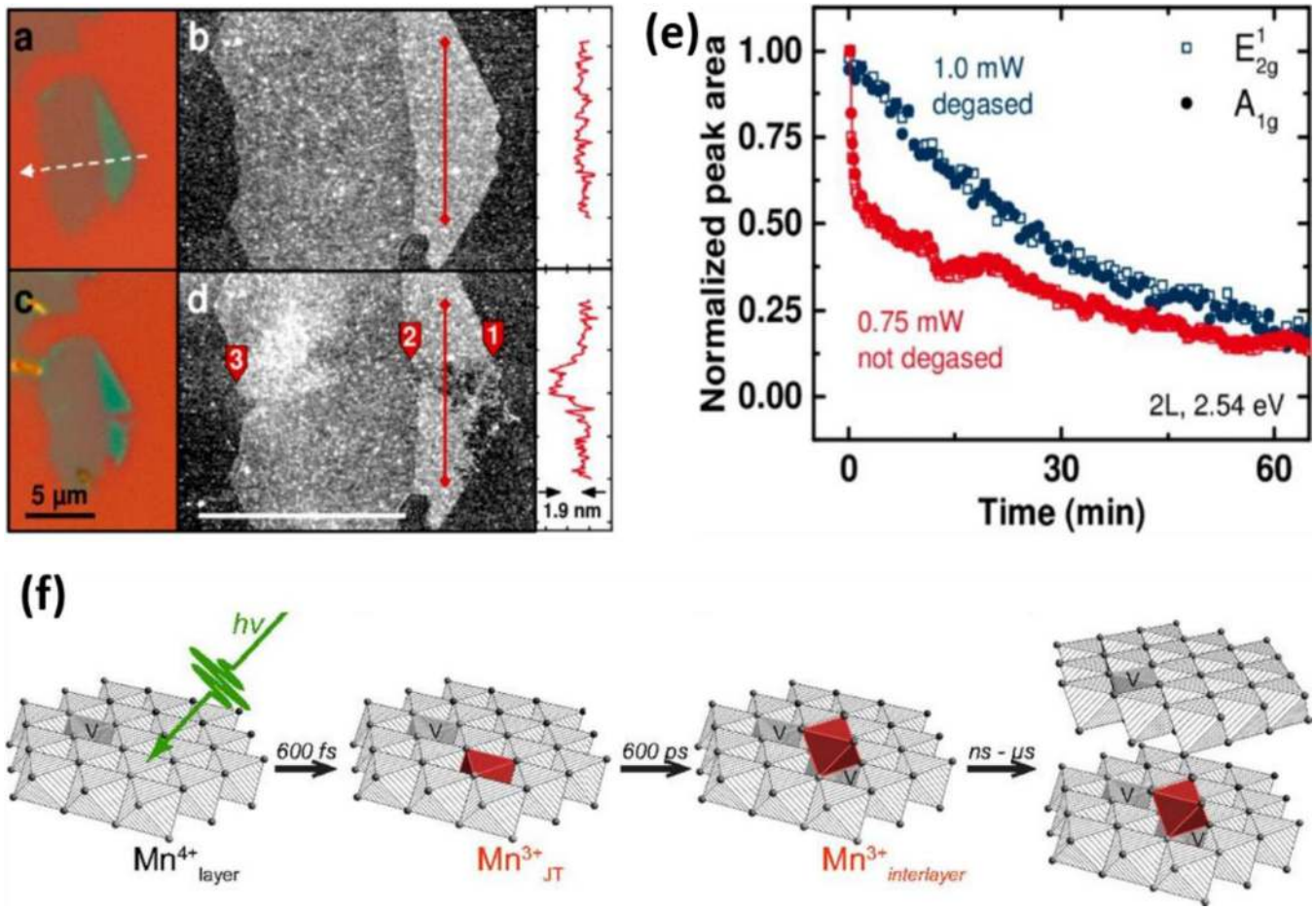


**Figure 11.**

(a, c) Optical microscopy (100×) and (b, d) AFM image of exfoliated $MoS_2$ nanosheets before (top) and after (bottom) laser line scan, showing edge sites are the primary targets of photodegradation. e) Normalized Raman peak area as a function of illumination time on the edge site of a bilayer flake in the electrolyte with reduced oxygen (blue) and natural amount of dissolved oxygen (red). Reprinted with permission from ref. 214. Copyright 2015 American Chemical Society. (e) Proposed model for the evolution of redox chemistry in the photoreduction of $MnO_2$ monolayer including photon absorption, formation of distorted Mn (III), migration of Mn(III) to an adsorption site and increased nanosheet stacking. Copyright (2015) National Academy of Sciences, USA.

## Table 1

Toxicity of 2D Materials and their Compound Materials

| Materials | Exposure Method | Species/Cell Types | Biological Outcomes | Literature |
|---|---|---|---|---|
| | | ***2D and 2D Layered Materials*** | | |
| $MnO_2$ | cell culture | Human breast cancer cells (MCF-7) | ~45 % viability after exposure to 100 ppm PEG coated nanoplates (width 20–70 nm) for 24 h | 128 |
| $MoO_3$ | cell culture | Human breast cancer cells (iMCF-7 and MCF-7) | ~ 40–50 % viability after 48 hr exposure to 400 ppm as-prepared nanoplates (400 nm × 100–200 nm) | 127 |
| $TiO_2$ | IP injection | mice (C57) | PEG coated $TiO_2$ nanosheets (anatase, lateral dimension 92.5 nm) accumulate in liver and spleen and cause appreciable toxicity in liver at 10 μg/g-body weight. | 126 |
| $WS_2$ | cell culture | mouse mammary gland cancer cells (4T1), Human Cervix cancer cells (Hela), human kidney cancer cells (293T) and human lung cancer cells (A549) | ~ 50% viability for 4T1, Hela, 293T after 24 hr exposure to 100 ppm nanosheets; ~30% viability for A549 after 24 hr exposure to 400 ppm nanosheets (lat. dim. ~500 nm, thickness ~20 nm) | 129111 |
| $MoS_2$ | cell culture; oropharyngeal aspiration | human Cervix cancer cells (Hela) and human lung cancer cells (A549); *Escherichia coli* (*E. coli*) K12; human leukemia monocytes (THP1) and human lung cells (BEAS-2B) and C57Bl/6 mice; rat kidney cells (RAMEC) and rat Adrenal Gland cells (PC-12) | ~70–95% viability for Hela cells exposed to 160 ppm PEGylated nanosheets (50nm × 2nm); ~50% viability for A549 cells exposed to 400 ppm nanosheets (~400x~4.5 nm); cell viability decreases as extent of exfoliation increases in panel of $MoS_2$ nanosheets; Aggregated but not dispersed $MoS_2$ nanosheets induce acute lung inflammation in mice; no loss of viability in RAMEC and PC 12 cells exposed to few-layer $MoS_2$ nanosheets at doses up to 100 μg/ml. | 110–113, 119, 123 |
| $WSe_2$ | cell culture media | human lung cancer cells (A549) | ~30 % viability for A549 after exposure to 400 ppm as-exfoliated materials (lateral dimension ~200 nm, thickness ~7 nm) for 24 hrs | 111 |
| $Bi_2Se_3$ | cell culture media; IP injection | mouse liver cancer cells (H22); male mice (C57) | ~90 % viability for hepatocarcinoma H22 cells after exposure to 200 ppm PVP-coated nanosheets (rhombohedral phase, lateral dimension 90 nm, outer layer 3.6 nm, inner thickness 21 nm) for 24, 48, 72 h; IP injection of PVP-coated $Bi_2Se_3$ nanosheets (50 nm × 6 nm) in mice at doses up to 20 mg/kg produced no obvious adverse effects on growth or changes in body weight up to 90 days, and a panel of measurements focused on immune response, hematology, and biochemistry suggested “limited biological damage” | 125, 130 |
| $TiS_2$ | cell culture media and intravenous injection | mouse mammary gland cancer cells (4T1); mice (Balb/c) | No obvious toxicity with up to 100 pm $TiS_2$-PEG nanosheets (cubic phase, lateral dimension ~100 nm) to 4T1 cells and no obvious damage to mouse organs up to the 2 mg/mL, 200 μl TiS2-PEG injection (20 μg/g-body weight) | 124 |
| | | ***Other Nanomaterials Forms (Particulate or Fibrous)*** | | |
| $MnO_x$ | Inhalation; cell culture | rats (Fischer 344); rat liver fibroblasts (BRL 3A) | Manganese oxide nanoparticles (30 nm) altered gene expression in olfactory bulb, frontal context, midbrain, striatum, cerebellum rats after 11 days of inhalation; 60% viability for BRL 3A cells exposed to 250 ppm particles for 24 h. | 131132 |
| h-BN | cell culture | human embryonic kidney cells (HEK293); rat adrenal gland cells (PC-12) | Nontoxic up to 100 ppm for HEK293 cells after exposure to h-BN multiwalled nanotubes (diameter 20–30 nm, | 133, 134 |

| Materials | Exposure Method | Species/Cell Types | Biological Outcomes | Literature |
|---|---|---|---|---|
| | | | length up to 10 mm) for 4 days; 20% decrement of metabolic activity for PC12 cells after exposure to 100 ppm bamboo-like nanotubes (diameter 50 nm, length 200–600 nm) for 9 days. | |
| $MoS_2$ | cell culture | human lung cancer cells (A549), human bone marrow leukemia cells (K562), human embryonic skin fibroblasts (CCC-ESF-1) | No cytotoxicity for A549, K562, CCC-ESF-1 cells after exposure to 3.5 ppm nanoparticles (hexagonal phase, 120 nm) for 48 h | 135 |
| $MoO_3$ | cell culture | rat fibroblasts (BRL 3A); human bone osteosarcoma cells (U2OS ) | ~ 60 or 50 % layered double hydroxide (LDH) leakage and ~20 or ~40 % viability for BRL 3A cells after exposure to 250 ppm nanoparticles (30 or 150 nm) for 24 h; No cytotoxicity for U2OS cells after exposure to 4 ppm nanospheres (290.4 ± 66.7 nm) for 2 h; | 132, 136 |

**Table 3**

Relevant Mechanical Properties of 2D Materials and Biological Structures

| | Bending stiffness $\kappa$ ($k_BT$) | In-plane Young's modulus $Y^{2D}$ /area extension modulus $K_A$ (J/m$^2$)[a] | Breaking strength/lysis tension (J/m$^2$)[b] | Thickness $h$ (nm) | Poisson ratio $\nu$ |
|---|---|---|---|---|---|
| Graphene monolayer | 56 [286, 287] | 340 [286, 288] | 42 [288] | 0.32 [289] | 0.17 [288, 289] 0.149 [286] |
| h-BN monolayer | 37 [290] | 271 [286, 291]; 292 [292] | 27.8 [291]; 71.7 [292] | 0.32 [293] | 0.211[286, 291] |
| $MoS_2$ monolayer | 375 [294] | 180±60 [295, 296] | 15±3 [295] | 0.65 [295, 297] | 0.3 [296] |
| $MoS_2$ bilayer | 700[c] | 260±70 [295] | 28±8 [295] | 1.3 | 0.3 |
| Graphyne monolayer | 65 [298] | 166 [299, 300] | 20.64 [300] | 0.32 [298] | 0.42 [299, 300] |
| GO monolayer with carbon-to-oxygen ratio (4:1) | 183[d] | 270 [301] | 17–22 [301] | 0.7 [302] | 0.165 [302] |
| Lipid bilayer membrane[e] | 10–20 [282, 303] | 0.25 [303, 304] | on the order of 0.001 J/m$^2$ [305, 306] | 4–5 [282] | N/A |
| Plasma membrane of red blood cell[f] | 50–100 [282, 307] | 0.45 [282] | on the order of 0.001 J/m$^2$ [305, 306] | 4–5 [282] | 0.33 [308] |

[a] The in-plane Young's modulus $E^{2D}$ of solid 2D materials, representing material resistance against in-plane deformation, is defined as $E^{2D}=E_b h$, where $E_b$ is the bulk Young's modulus of a three-dimensional stack of layers spaced at $h$.

[b] The lysis tension is the maximum biaxial tension a lipid bilayer membrane can sustain before rupture.

[c] The bending stiffness of $MoS_2$ bilayer is usually expressed as $\kappa=E^{2D}h_S^3/[12(1-\nu^2)]$ according to the conventional theory of plates and shells, where the in-plane Young's modulus $E^{2D}$ is taken to be 260 J/m$^2$, Poisson ratio $\nu=0.3$, and thickness $h_S=0.62$ nm.[286]

[d] Mechanical properties of a GO monolayer depend on its atomic structure and chemical composition such as carbo-to-oxygen ratio.

[e] Although the bending rigidity of a lipid bilayer falls typically in the range $\kappa=10–20\ k_BT$, it can vary from 10 $k_BT$ to 150 $k_BT$ depending on the membrane composition.

[f] The plasma membrane of a red blood cell consists of a bilayer of phospholipids, cholesterol molecules, transmembrane proteins and an underlying spectrin network which is attached to the membrane. Poisson ratio of the plasma membrane can be attributed to that of the spectrin network which is typically taken as $\nu=0.33$.